Accepted for publication in the Astrophysical Journal

The Spectrum and Variability of Circular Polarization in Sagittarius A* from 1.4 to 15 GHz

Geoffrey C. Bower[1,2], Heino Falcke[3], Robert J. Sault[4] & Donald C. Backer[2]

ABSTRACT

[1]National Radio Astronomy Observatory, P.O. Box O, 1003 Lopezville, Socorro, NM 87801; gbower@nrao.edu

[2]Astronomy Department & Radio Astronomy Laboratory, University of California, Berkeley, CA 94720; gbower,dbacker@astro.berkeley.edu

[3]Max Planck Institut für Radioastronomie, Auf dem Hügel 69, D 53121 Bonn Germany; hfalcke@mpifr-bonn.mpg.de

[4]Australia Telescope National Facility, P.O. Box 76, Epping, NSW, 1710, Australia ; rsault@atnf.csiro.au

We report here multi-epoch, multi-frequency observations of the circular polarization in Sagittarius A*, the compact radio source in the Galactic Center. Data taken from the VLA archive indicate that the fractional circular polarization at 4.8 GHz was -0.31% with an rms scatter of 0.13% from 1981 to 1998, in spite of a factor of 2 change in the total intensity. The sign remained negative over the entire time range, indicating a stable magnetic field polarity. In the Summer of 1999 we obtained 13 epochs of VLA A-array observations at 1.4, 4.8, 8.4 and 15 GHz. These observations employ a new technique that produces an error of 0.05% at 1.4, 4.8 and 8.4 GHz and 0.1% at 14.9 GHz. In May, September and October of 1999 we obtained 11 epochs of Australia Telescope Compact Array observations at 4.8 and 8.5 GHz. In all three of the data sets, we find no evidence for linear polarization greater than 0.1% in spite of strong circular polarization detections. Both VLA and ATCA data sets support three conclusions regarding the fractional circular polarization: the average spectrum is inverted with a spectral index $\alpha \approx 0.5 \pm 0.2$; the degree of variability is roughly constant on timescales of days to years; and, the degree of variability increases with frequency. We also observed that the largest increase in fractional circular polarization was coincident with the brightest flare in total intensity. Significant variability in the total intensity and fractional circular polarization on a timescale of 1 hour was observed during this flare, indicating an upper limit to the intrinsic size during outburst of 70 AU at 15 GHz. The fractional circular polarization at 15 GHz reached -1.1% and the spectral index is strongly inverted ($\alpha \sim 1.5$) during this flare. We tentatively conclude that the spectrum has two components that match the high and low frequency total intensity components.

Subject headings: Galaxy: center — galaxies: active — polarization — radiation mechanisms: non-thermal — scattering

1. Introduction

The compact radio source in the Galactic Center, Sagittarius A*, is the best and closest candidate for a supermassive black hole in the center of a galaxy (Maoz 1998; Melia & Falcke 2001). The source Sgr A* is positionally coincident with a $\sim 2.6 \times 10^6 M_\odot$ dark mass (Genzel et al. 2000; Ghez et al. 2000). Very long baseline interferometry (VLBI) has shown that this source has a scale less than 1 AU and a brightness temperature in excess of 10^9 K (Rogers et al. 1994; Bower & Backer 1998; Lo et al. 1998; Krichbaum et al. 1998; Doeleman et al. 2001). However, strong interstellar scattering of the radiation along the line of sight has

been shown to broaden the image of Sgr A* at radio through millimeter wavelengths (**?**, e.g.,)]1998ApJ...508L..61L,1994ApJ...427L..43F. As a consequence, VLBI observations have not convincingly demonstrated the existence of source structure that would be an important diagnostic of physical processes. Long-term studies of Sgr A* indicate that the source shows no motion with respect to the center of the Galaxy (Backer & Sramek 1999; Reid et al. 1999). For these reasons, it is inferred that Sgr A* is a synchrotron or cyclo-synchrotron emission region powered through accretion onto a supermassive black hole (Melia 1994). Significant details of the emission mechanism are not understood. In particular, leading models propose that the emission originates in an advection dominated accretion flow, or ADAF (Özel et al. 2000); in a convection dominated accretion flow, or CDAF (Quataert & Gruzinov 2000b); or, in an outflow or jet (Falcke et al. 1993; Falcke & Markoff 2000).

Polarization has proved to be an important tool in the study of AGN. Studies of linear polarization (LP), which is typically on the order of a few percent or less of the total intensity, have confirmed that the emission process is synchrotron radiation and demonstrated that shocks align magnetic fields in a collimated jet, leading to correlated variability in the total and polarized intensity (Hughes et al. 1985; Marscher & Gear 1985). Circular polarization (CP), on the other hand, is less well understood in AGN. Typically, the degree of CP is $m_c < 0.1\%$ with only a few cases where m_c approaches 0.5% (Weiler & de Pater 1983; Rayner et al. 2000). The degree of CP usually peaks near 1.4 GHz and decreases strongly with increasing frequency.

Recently, VLBI imaging of several AGN has found localized CP (Homan & Wardle 1999). In 3C 279, these authors found $m_c \simeq 1\%$ in an individual radio component with a fractional LP of 10% (Wardle et al. 1998). The integrated CP, however, is less than 0.5%. CP was also discovered in the radio jet of the X-ray binary SS 433 at a level comparable to that of the LP (Fender et al. 2000). The galactic microquasar GRS 1915+105 also shows strong and variable CP that is associated with jet ejections (Fender et al. 2001). The CP in these sources is probably produced through the conversion of LP to CP by low-energy electrons in the synchrotron source. This process is also known as repolarization (Pacholczyk 1977). CP has been identified through surveys in a number of high luminosity AGN (Rayner et al. 2000; Homan et al. 2001). A survey of low luminosity AGN found CP in only 1 of 11 galaxies, M81* (Brunthaler et al. 2001). This discovery is of particular interest to this paper because of the similarity of M81* and Sgr A*, including the absence of LP.

In recent interferometric work we have shown that the LP of Sgr A* from centimeter to millimeter wavelengths is extremely low. LP was not detected in a spectro-polarimetric experiment with an upper limit of 0.2% for rotation measures as large as 10^7 rad m^{-2} at 8.4 GHz (Bower et al. 1999a). More recently, we have found that LP is less than 0.2% at 22

GHz and less than $\sim 1\%$ at 112 GHz (Bower et al. 1999c, 2001). Interstellar depolarization is very unlikely within the parameter space covered by these observations. Aitken et al. (2000) have claimed LP of $\sim 10\%$ at $\nu \geq 150$ GHz on the basis of low resolution JCMT observations. If these results hold, then they have significant implications for models of the emission mechanism (Quataert & Gruzinov 2000a; Agol 2000; Melia et al. 2000).

Given these stringent limits on LP, the presence of CP is not expected. Nevertheless, we have detected CP at a surprisingly high level (Bower et al. 1999b; Sault & Macquart 1999). We found the fractional CP $m_c = -0.37 \pm 0.04\%$ at 4.8 GHz and a spectral index $\alpha \sim -0.5$ between 4.8 and 8.4 GHz ($m_c \propto \nu^\alpha$). Simple synchrotron models cannot produce the full polarization characteristics without depolarization or repolarization in the source or in the accretion region. The introduction of low energy electrons may lead to these Faraday effects and/or strong gyrosynchrotron emission, which exhibits strong CP (Ramaty 1969). Interstellar scattering in a magnetized plasma may also lead to CP in radio sources (Macquart & Melrose 2000).

We describe here VLA and ATCA observations of CP and LP in Sgr A*. Because of the technical difficulties and the novelty of these observations, especially for the VLA, we emphasize the technique and the sources of error in our discussion. In §2, we discuss the analysis of 20 y of archival VLA data at 4.8 and 8.4 GHz. These data show that the CP is stable over this period. In §3, we summarize new VLA observations in the Summer of 1999 at 1.4, 4.8, 8.4 and 15 GHz. We discuss sources of error in these data in §4. In §5, we introduce new ATCA observations from 1999 at 4.8 and 8.5 GHz. These observations have very different systematic errors from those of the VLA. We consider the long-term evolution of CP in Sgr A* in §6 based on results from the archival VLA data. We analyse the new VLA and ATCA data in §7 and §8. This includes demonstration of consistency between the various data sets and statistical measures of variability. We discuss our results in §9 and summarize our conclusions in §10.

2. VLA Archive Observations and Results

We reduced data of Sgr A* taken from the VLA archives. All observations were taken from the proper motion data sets of Backer & Sramek (1999). These observations had similar characteristics to those that we reported in Bower et al. (1999b), which were the final epoch of the Bower et al. (1999b) proper motion study. Further details of the observations are given in Bower et al. (1999b).

All observations were made in the A array. Eight epochs of observation were made,

each consisting of two or three five-hour runs spaced over a few weeks. Data sets before 1989 include only 4.8 GHz observations. Data sets from 1989 onward include a small amount of 8.4 GHz observations. Each data set has observations of Sgr A*, W56 (J1745-2820), W109 (J1748-2907), GC 441 (J1740-2930), J1743-0350 and J1751-2523. Sgr A*, W56, W109 and GC 441 were observed multiple times within an hour. J1743-0350 and J1751-2523 were observed hourly.

Data reduction was performed with AIPS. *A priori* amplitude calibration was done using a single observation of 3C 286. Amplitude gains were determined with J1743-0350. At 4.8 GHz, we also calibrated the LP. Polarization leakage terms were determined using J1743-0350. Polarization position angles were calibrated with 3C 286. Polarization calibration failed for unknown reasons on 4 February 1989 and 24 April 1998 and these data were excluded from further analysis. The parallactic angle coverage at 8.4 GHz was too limited to permit accurate leakage term calibration. Amplitude gains and leakage terms were transferred from J1743-0350 to the other sources. These sources were then phase-only self-calibrated and imaged in Stokes I, Q, U and V at 4.8 GHz and Stokes I and V at 8.4 GHz. Fluxes were determined by fitting a beam-sized Gaussian at the image center. All self-calibration and imaging were performed using baselines longer than 100 $k\lambda$ at 4.8 GHz and 150 $k\lambda$ at 8.4 GHz in order to exclude contamination from extended structure.

The results are summarized Figures 1 to 9 and Table 2. Figures 1 and 3 give the measured fractional CP for each source at 4.8 and 8.4 GHz, respectively. The plotted errors are the results of thermal noise. We see clearly in these that there is an apparent variation common to all sources. This indicates that some component of the measured signal is in fact due to instrumental error or due to variable CP in the amplitude calibration source, J1743-0350. We can estimate the degree of this variation with the assumption that the sources W56, W109 and J1751-2523 are unpolarized. The source GC 441 is probably also unpolarized but the limits on fractional polarization in this source are too high because of its low flux density. We estimate the correction as the mean of the fractional CP for W56, W109 and J1751-2523. This correction is subtracted from the raw fractional CP of each source (Figures 2 and 4). The corrections are shown in Figure 5. The application of the correction flattens the light curve in fractional CP for Sgr A*. It also reduces the scatter between results for Sgr A* in 6 of 8 epochs at 4.8 GHz (Figure 5). We estimate the error with the rms scatter, which is on the order of 0.1%. This is consistent with the theoretical estimate of the error from our analysis in §4. The results of April 1998 published in Bower et al. (1999b) are more negative by $\sim 0.1\%$.

Figures 6 and 7 show the total intensity at 4.8 and 8.4 GHz, respectively. Figures 8 and 9 show Stokes Q and U at 4.8 GHz. Plotted errors are thermal noise. Sensitivity limits for

Q and U are set at 0.1% by variations in the polarization leakage terms (Holdaway et al. 1992).

3. VLA Observations in 1999

Sgr A* was observed by the VLA in the A array on 13 occasions in 1999. These observations were spaced roughly by one week covering the time range 23 June 1999 to 21 September 1999. The shortest and longest gaps between observations were 5 and 18 days, respectively. Each observation was approximately 4 hours in length.

On all but one day, observations were made at 1.4, 4.8, 8.4 and 15 GHz. On 30 June 1999, observations were not made at 15 GHz. All observations were made with 50 MHz bandwidth in left (LCP) and right (RCP) circular polarization.

Observing was divided into 5 blocks. Each block consisted of a 1.4 GHz segment and a 4.8, 8.4 and 15 GHz segment. Each segment began with a pointing scan on J1733-1304 at 1.4 GHz or 8.4 GHz. Separate pointing scans were necessary because of the uncertain alignment of the 1.4 GHz feed with the higher frequency feeds. The segments continued with observations of J1733-1304, Sgr A*, J1751-2523 and J1744-3116 at each frequency. The higher frequency feeds are collimated with each other. J1751-2523 was not observed at 15 GHz due to its steep spectrum.

A priori amplitude calibration was performed with the source 3C 286 at all four frequencies. Self-calibration on J1733-1304 determined antenna-based amplitude gains. These gains were transferred to the other sources. LP calibration was performed with J1733-1304. Electric vector position angle calibration was performed using 3C 286. All program sources were phase-only self-calibrated and then imaged in Stokes I, Q, U and V. Fluxes were determined by fitting a beam-sized Gaussian at the image center. All self-calibration and imaging were performed using baselines longer than 100 $k\lambda$ at frequencies higher than 4.8 GHz and baselines longer than 30 $k\lambda$ at 1.4 GHz in order to exclude contamination from extended structure. Data from 10 August 1999 were corrupt and not used.

We tabulate the mean total intensity and fractional CP in Tables 1 and 2. We show in Figures 10 and 11 the results. Figure 10 shows Stokes V at all four frequencies for the three target sources, Sgr A*, J1751-2523 and J1744-3116. Figure 11 shows the total intensity evolution for the three target sources. We do not plot LP results but they clearly show no LP for Sgr A* at all four frequencies at a level of $\sim 0.1\%$ on all dates. LP measured for J1751-2523, J1744-3116 and J1733-1304 were slowly variable.

4. Error Analysis of VLA CP Measurements

The VLA is equipped with RCP and LCP receivers. Stokes V is measured as the difference between the correlated parallel hands in polarization, i.e. $V = 1/2(RR - LL)$. Errors in CP measurements with the VLA have seven origins: one, thermal noise; two, gain errors; three, beam squint; four, second-order leakage corrections; five, unknown calibrator polarization; six, background noise; and seven, radio frequency interference. Primarily, the first four of these are stochastic and the last three are systematic. Our stochastic noise model is parametrized by N, the number of 2.5 minute scans, and N_a, the number of antennas (Table 3). For the monitoring observations, $N = 5 \pm 1$. For the archive data, $N \approx 12$ at 4.8 GHz and $N \approx 4$ at 8.4 GHz. We discuss each of the noise sources individually and then compare the predictions of our model to the actual measurements. The agreement is good.

4.1. Thermal Noise

Receiver noise introduces an error that is inversely proportional to $\sqrt{N_a(N_a - 1)BN}$, where $B = 50$ MHz is the observing bandwidth. For $N = 5$ at 8.4 GHz, the error for the VLA is 40 μJy, or 0.005% for Sgr A*. This is an insignificant source of error for our VLA results.

4.2. Gain Errors

Calibration can introduce a significant error in CP measurements. This can occur in two ways: one, the amplitude calibration source is too weak for accurate gain measurement; two, the amplitude gains determined for the calibrator are not the same as the gain on the target source. Any errors in our observations are due to the latter. The primary amplitude calibrators, J1743-0350 and J1733-1304, have flux densities on the order of 4 Jy, implying that the SNR of amplitude calibration is on the order of 10^5 for a 2.5-minute scan.

We cannot easily separate the effects of errors from gain variation with sky angle and errors from gain variation with time. However, both errors will likely have a similar signature in RCP and LCP, reducing their effect significantly. Furthermore, the gain curves for VLA antennas are known to be flat at these frequencies, although to what degree is uncertain. Significant gain errors in angle would appear as a systematic shift in the flux densities of the target sources, which is not seen. We can estimate the combined effect of gain variations in time and angle by measuring the variation of the gain solutions. We find from our solutions that the antenna gain variations are typically 0.3%. The total error is inversely proportional

to $\sqrt{N_a N}$, which is on the order of 0.03%.

4.3. Beam Squint

Beam squint is the result of offset RCP and LCP receivers in the VLA antennas (Sault et al. 1991). This introduces a false CP off the beam axis. Pointing errors can, therefore, lead to false CP. In Figure 12, we show the false CP induced due to beam squint for a single antenna and for the array, for pointing errors of $10''$ (uncorrected pointing) and $2''$ (best case of reference pointing). The error due to beam squint scales inversely with $\sqrt{N_a N}$, if pointing errors are uncorrelated. Rejection of antennas with large amplitude variations is an important step before imaging for reducing the effect of beam squint. A small number of antennas with known pointing problems were routinely rejected.

4.4. Second-Order Leakage Terms

Perfect receivers are sensitive to only a single polarization. Real receivers are sensitive to both LCP and RCP. A complete treatment of this polarization leakage leads to an identification of second-order terms that affect Stokes V (**?**, e.g.,)]1994ApJ...427..718R. These terms are proportional to $|D|^2 I$ and DP, where I is the total intensity, P is the LP intensity and D is the leakage fraction. $|D|$ is on the order of a few percent for the VLA. For the observed sources, $P/I \sim 1\%$. For Sgr A*, $P/I < 0.1\%$. The sum of these terms contributes approximately 0.03%.

4.5. Unknown Calibrator Polarization

This is a systematic error that is introduced in the calibration step. For self-calibration, we assume that the calibration source is unpolarized. The target source polarization will then be offset from its true value by the calibrator polarization. A strongly polarized calibrator will be detectable as a systematic offset in the target sources. This may have played a role in the correction factor applied to the archive data. We show below absolutely determined CP for our calibrator sources from ATCA. These are all on the order of 0.1% or less. This is probably the dominant source of systematic error in the VLA measurements.

4.6. Background Noise

The strong background in the Galactic Center can introduce false CP. This is a systematic error that is due to nonlinearity in the amplifier chains. These are known to be linear to better than 1%. This effect is greatest at low frequencies, where the background is brightest. At 4.8 GHz, the shift in system temperature between Sgr A* and a calibrator source is from 35 to 25 K. This implies an error $\lesssim 0.3\%$ per polarization per antenna. Averaging, we find a total systematic offset of $\lesssim 0.04\%$. The sign of this offset is unknown.

4.7. Interference

Interference can also introduce errors in CP. Many satellite and terrestrial beacons radiate in only a single circular polarization. Many of our observations are not made fully in protected radio bands. Interference as a source of CP can be identified if the CP for several nearby sources is similar or if the CP is time-variable. Our consistent detections for Sgr A* at multiple frequencies and non-detections for calibrator sources argue against interference errors.

4.8. Comparison with Measured Errors

We can estimate the actual error in CP by measuring variations in the CP observed for the calibrator sources. The best estimate of the noise in an individual measurement is the rms difference between two consecutive measurements. In an evenly sampled data set this is the structure function of CP evaluated on the shortest sampling time scale. We summarize in Table 4 these values for Sgr A*, J1744-3116 and J1751-2523. The variations for J1751-2523 are the lowest and, therefore, the most indicative of the noise level at 1.4, 4.8 and 8.4 GHz. The measured values are within 50% of the estimated values (Table 3), confirming our error model. At 15 GHz, the measured variations for J1744-3116 are 0.14%, significantly higher than estimated. There is probably a substantial component from intrinsic variation in J1744-3116, which is apparent at the 0.10% level at the lower frequencies. This implies that the true error at 15 GHz is on the order of 0.10%.

5. ATCA Observations in 1999

We observed Sgr A* with ATCA in the Spring and Fall of 1999. These observations are an important complement to the VLA observations because they have an entirely different set of systematic errors associated with them. Most importantly, the ATCA receives orthogonal linear polarizations. The CP is formed from the sum of correlated cross-hand visibilities rather than from the difference of correlated parallel-hand visibilities. The result is insensitive to amplitude calibration, beam squint, and calibrator polarization. Furthermore, the differences in antenna size and shape, array configuration and location provide a test against effects of background, second-order leakage term and interference. Additionally, separate calibrators and analysis techniques were used. The errors are dominated by thermal effects and leakage term measurements.

Standard polarization observation and reduction techniques are described in Sault et al. (1991). These methods have been shown to produce errors in CP $\sim 0.01\%$. All analysis was performed with the MIRIAD software Sault et al. (1995). We observed the source B1934-638 to calibrate amplitudes and to determine leakage terms. The compact source J1820-2528 was observed to determine the time-dependent phase solutions. These were applied to Sgr A* and other calibrators. Observations were performed in the extended 6A and 6D configurations of the ATCA, which have a maximum baseline of 6 km. Only baselines longer than 30 $k\lambda$ were used in analysis of Sgr A*. This smaller limit on the baseline length is necessary because of the more compact configuration of the ATCA.

Observations in the boreal Spring of 1999 were conducted on 11 May, 22 May and 02 June. These observations were each 12 h tracks on Sgr A*. Sky frequencies were centered at 4.8 GHz and 8.6 GHz with 128 MHz of bandwidth in two polarizations at each frequency. Several calibrators were observed in addition to J1820-2528. Limited observations of J1751-2523, J1733-1304, J1743-038, W56, W109 and GC 441 were also made.

Observations in the boreal Fall of 1999 were made on 8 dates between 11 September and 04 October. Typical tracks were 6h in duration. The sky frequencies were 8.512 GHz and 8.640 GHz with 128 MHz bandwidth at each frequency. Again, J1820-2528 was used as the main phase calibrator. J1744-3116 and J1751-2523 were also routinely observed

We plot in Figures 10 and 11 the results of the ATCA observations for Sgr A*, J1744-3116 and J1751-2523. Mean CP is listed in Table 2 for all sources. We also produced LP results which are consistent with the VLA results.

We have a few ATCA measurements of the CP in our VLA calibrators J1733-1304 and J1743-038. These low values confirm that the CP in these sources does not strongly bias the VLA results.

6. Timescales Greater than 1 Year

From the VLA archive data we see that the CP of Sgr A* is roughly constant over 18 y. The mean is $m_c = -0.31 \pm 0.13\%$ at 4.8 GHz and $m_c = -0.36 \pm 0.10\%$ at 8.4 GHz. The errors are measures of scatter. Because of our reduction methods, we cannot make any statements about variability within an epoch. However, we can estimate whether there is variability between epochs if we estimate the error in m_c for each epoch as the scatter in the measurements added in quadrature with a systematic error of 0.05%. Under the assumption of constant m_c, the reduced χ^2 is 1.6 at 4.8 GHz and 1.1 at 8.4 GHz. This is consistent with constant m_c for the typical error of 0.1% on timescales longer than 1 y and less than 18 y. The mean spectral index is slightly inverted. We find for $m_c \propto \nu^\alpha$, $\alpha = 0.2 \pm 0.7$.

The constant fractional CP occurs simultaneously with a slow change in the total intensity. The total intensity decreases by a factor of ~ 2 in the 18 y period. We find no evidence for LP in Sgr A* at 4.8 GHz above 0.1% over 18 y.

7. Timescales Between 1 Day and 1 Year

We can use the VLA and ATCA observations to constrain the degree of variability of CP in Sgr A* on timescales between 3 and 100 days. We can also use the VLA data to characterize the spectral evolution of variability from 1.4 to 15 GHz on these timescales. There is good agreement between the results from the VLA and ATCA at 4.8 and 8.4 GHz.

First, we discuss the nature of total intensity variability in Sgr A*. We can construct a structure function from the VLA and ATCA data. The structure function is defined as

$$D^2(\tau) = \frac{1}{T} \int_0^T dt \left[S(t+\tau) - S(t) \right]^2 . \quad (1)$$

In order to compute this continuous function for our discretely and irregularly sampled data, we calculate the difference for each pair of points and average them in bins. We plot for both sources the structure function of total intensity (Figure 13). Variability increases strongly with frequency. We also see that the structure function rises with τ on timescales of 3 to 100 days at all frequencies. At 4.8 GHz, the structure function continues to increases out to > 1000 days. These results echo the earlier conclusions of Zhao et al. (1992), Backer (1994) and Falcke (1999).

From the CP data, we draw several conclusions. One, the mean fractional CP spectrum is inverted. Two, the degree of variability increases with frequency. Three, the time scale for variability is as short as a few days to a week. Four, the largest change in fractional CP was coincident with the largest total intensity variation.

We plot in Figure 14 the mean spectrum and degree of variability of fractional CP in Sgr A*. The ATCA, VLA and VLA archive results are in good agreement at 4.8 and 8.4 GHz (Table 2). The mean spectrum in the Summer of 1999 is inverted with $\alpha = 0.5 \pm 0.2$. This figure demonstrates the increasing degree of variability with frequency. The degree of variability at 1.4 GHz is consistent with the noise, while the degree of variability at 15 GHz is three times greater than the degree of variability for J1744-3116 (Table 2).

We derive the structure function for the fractional CP in a similar manner to that of the total intensity. The structure functions for Sgr A* and J1744-3116 are plotted in Figure 15. These structure functions demonstrate a number of our conclusions. One, the increasing degree of CP variability with frequency is again apparent in the VLA data. Two, the degree of CP variability at 4.8 GHz is constant on timescales of 10 to 1000 days. The degrees of CP variability at 1.4, 8.4 and 15 GHz are constant on timescales of 10 to 100 days. Three, episodic CP variability has a substantial impact. The ATCA CP structure function at 8.4 GHz is substantially lower than that of the VLA at 8.4 GHz. Presumably, this is due to one or two major flares during the VLA monitoring and the absence of such events in the ATCA time periods. Four, the ATCA data indicate that there is a sharp decrease in the degree of CP variability on timescales less than 10 days. This may be true at all times or it may be a consequence of the lower overall variability during the ATCA epochs. The VLA data are not sensitive to timescales much less than 7 days. The combined VLA and ATCA structure function at 8.4 GHz (not shown) is consistent with the structure function converging to the 4.8 GHz value on long timescales. Finally, the structure functions for Sgr A* are substantially greater than that of J1744-3116, emphasizing the reality of the variability. Results for J1751-2523 are qualitatively similar but several times weaker than those of J1744-3116. There is also good agreement between the ATCA and VLA results at 8.4 GHz for J1751-2523.

The VLA light curves indicate that 10 days is a characteristic timescale for the rise and decay of flares in total intensity and CP (Figures 10, 11 and 16). Between day 210 and 217, there is a jump in m_c from -0.1% to -1.1% at 15 GHz. This is followed by slow decline in m_c over 20 d before another, smaller jump in m_c appears. These events are not correlated with any change in m_c for J1744-3116. The change between day 210 and 217 is coincident with a significant flare in the total intensity of Sgr A*. The increase in m_c between day 240 and 246 does not appear to have a correlated change in total intensity but it is of a smaller magnitude.

With the sampling available, there is little evidence for a time delay between flares at 15 GHz and 8.4 GHz. The flare on day 217 is not apparent at frequencies below 8.4 GHz. However, the flare at day 246 does appear at 4.8 GHz, although it appears to be of lesser

magnitude at 15 GHz than the previous flare.

8. Timescales Less than 1 Day

We analyzed the 1999 VLA data on timescales of less than 1 day, as well. We computed the Stokes I and V terms for 30 second averages. The results clearly indicate episodic activity. On some days, there is no evidence for variability in either term. However, at the time of the peak flux density (day 217) we see a $\sim 20\%$ change in the total flux density over a period of two hours at 15 GHz (Figure 17). Similar, but less prominent changes are apparent at 8.4 and 4.8 GHz. The flux density at these lower frequencies does not clearly saturate in the way that it does at 15 GHz. No change is apparent at 1.4 GHz. A factor of two change in Stokes V is apparent at 15 GHz over the same time range with $\chi^2_\nu = 3.7$ (Figure 18). There is a delay between the onset of variability in Stokes I and Stokes V of at least 1 hour. No significant change is apparent at any other frequency in Stokes V due to a lack of sensitivity.

Short-term variability was convincingly seen ($\Delta I > 100$ mJy at 15 GHz) in only one other epoch. On day 204, the 15 GHz flux density increased by 150 mJy in two hours. The 8.4 GHz flux density also increased but by a lesser amount and no variability was detected at the lower frequency. There is no evidence for fluctuations in CP on this date.

We computed mean structure functions from the VLA data at a timescale of 1 hour for Sgr A* and J1744-3116 in total intensity and fractional CP (Figures 13 and 15). In total intensity, Sgr A* is significantly more variable than J1744-3116. The degree of variability increases with frequency as it does on longer timescales. The structure function increases roughly as $\tau^{1/2}$ from 1 hour to 100 days. That power law holds to ~ 3000 days at 4.8 GHz. The power law index is slightly larger than that found by Backer (1994). In fractional CP the structure function on short timescales is dominated by noise. The structure function for Sgr A* and J1744-3116 are similar at 1 hour. However, the structure for Sgr A* does increase between 1 hour and 10 days. The high fractional CP structure function at 1.4 GHz is due to the complex extended structure in the Galactic Center, which is not well-modeled on short intervals.

9. Discussion

We discussed in detail in Bower et al. (1999b) some of the difficulties in producing high CP and low LP at centimeter wavelengths with a synchrotron source. Interstellar propagation effects predict a very steep-spectrum behavior and are not very efficient (Macquart & Melrose

2000), so that they cannot be invoked as a major contibutor to the overall CP of Sgr A*. We conclude that the CP we measure is intrinsic to Sgr A*. The responsible mechanism then is either circular polarization from gyrosynchrotron emission (Ramaty 1969) or re-polarization/conversion of LP to CP (Pacholczyk 1977) — both processes are most efficient in the presence of low-energy electrons with Lorentz factors of only a few. The introduction of a high density region of non-relativistic electrons, either in the accretion region for $r < 0.01$ pc or in the source itself, can also lead to high depolarization factors needed to suppress the LP (Bower et al. 1999a; Quataert & Gruzinov 2000a).

Moreover, since the amplitude of total and polarized intensity variability is a function of frequency (Melia et al. 2000) single component, optically thin models (**?**, e.g.,)]1994AA...286..431D where all frequencies are produced at the same location and scale up and down together, cannot account for these properties. Inhomogenous, multi-component models must be used. This fits with the fact that conversion can produce very high degrees of CP in inhomogeneous sources with a range of spectral indices, including inverted and flat spectra (Jones & Odell 1977; Jones 1988).

One can split the total intensity spectrum of Sgr A* in two or three regimes. The millimeter/submillimeter has an excess of radiation compared to the cm-wave spectrum (Serabyn et al. 1997; Falcke et al. 1998). This bump is most likely associated with a very compact region near Sgr A*. In addition, the cm-wave spectrum of Sgr A* may also be separated in two regimes, above and below ~ 10 GHz, based on the fact that the variability behaviour seems to change (Falcke et al. 1998; Zhao et al. 2001).

We may be able to consider the CP spectrum as composed of two components, as well. The low frequency component may be determined from the spectrum on day 210 (Figure 16). This component has a spectral peak near 4.8 GHz and an index $\alpha \sim -0.5$ between 4.8 and 15 GHz. This component is apparently steady. The high frequency component is highly variable in the short term. The spectrum on day 217 indicates that the spectrum can be strongly inverted with $\alpha \approx 1.5$. The apparent decay time for this component is on the order of 20 days. The decay time is less than the decay time in total intensity, which is ~ 10 days.

If the higher frequency CP component is associated with the millimeter/submillimeter component, then the fractional CP of that component is much higher than the measured value. In a typical ADAF model, the millimeter/submillimeter component is modeled as thermal gyrosynchrotron emission. At 15 GHz, this thermal component contributes approximately 10% of the total intensity. This ratio holds roughly for the jet model (Falcke & Markoff 2000) as well as for the low $\dot{M}$ model of (Quataert & Gruzinov 2000a). Thus, the maximum CP at 15 GHz corresponds to $\sim -10\%$ of the total intensity of the millimeter/submillimeter component.

The coincidence of the brightest CP flare with the brightest total intensity flare suggests that the processes driving these phenomena are fundamentally linked. This flare occurred in phase with the 106 day period in total intensity (Zhao et al. 2001), suggesting that the CP may also be periodic. Since our CP data are only weakly sensitive to timescales of 100 days, we cannot confirm the periodicity in CP. However, sharper definition of the period phase and future CP observations will test this relationship more rigorously. Zhao et al. (2001) found that the periodic variability of Sgr A* at 15 GHz has an amplitude on the order of 30% of the total intensity. If the CP at 15 GHz is solely associated with this component, then it is $\sim -4\%$ polarized at its maximum.

An extrapolation of the high frequency CP spectrum at its peak flare state indicates that m_c may exceed 10% at 100 GHz. A single observation at 112 GHz found $m_c < 1.8\%$, indicating that if it does reach 10%, it does so episodically (Bower et al. 2001).

The long-term stability of m_c at 4.8 GHz combined with a factor-of-two change in total intensity suggests a linear relationship between CP and total intensity. A propagation effect such as birefringent scattering (Bower et al. 1999b; Macquart & Melrose 2000) could produce this relationship although it has difficulty accounting for the relatively flat spectrum of the CP. Simple synchrotron emission will produce this effect, too. This requires uniformity in the magnetic pole and accretion conditions over 20 y. Timescales for turbulence in the wind-driven accretion region are on this order of magnitude (Coker et al. 1999). This is a much more interesting limit on the stability of the handedness of CP than the 20 y limit found for luminous AGN, since intrinsic timescales typically scale with the mass of the black hole (Homan et al. 2001). On the other hand, the short timescale variations in GRS 1915+105 probe a very different accretion regime (Fender et al. 2001).

The power law index of the total intensity structure function also emphasizes the differences between Sgr A* and high luminosity AGN. Hughes et al. (1992) found no sources with a power law index less than 0.7 on timescales of months to ~ 10 years. These differences are not only the result of mass differences (if timescales scale linearly with mass). Our structure function timescales of 1 hour to 100 days would correspond to 1 month to 300 years. Thus, we conclude that variability on short timescales is qualitatively different from that of high luminosity AGN.

Variability in total intensity and in circular polarization appears to occur on a continuum of timescales from 1 hour to > 1000 days. The 1-hour timescale is comparable to the timescale for a ~ 50 times flare observed at X-ray wavelengths (Baganoff et al. 2001). The substantially lower amplitude of the radio variability probably implies an inverse-Compton origin for the X-ray photons (Markoff et al. 2001).

We can estimate an upper limit to the size of Sgr A* at 15 GHz given $\sim 20\%$ variability over 2 hours. An upper limit to the size of the outburst is then $c \times 2$ h/0.2 ~ 70 AU, which is 8 mas at the Galactic Center. This is larger than the 15 GHz scattering size of Sgr A* (5.4 mas). The observed source size will be 10 mas. If the source does grow to this upper limit size, then it could be readily detected with VLBI at 15 GHz and higher frequencies even if the intrinsic size is proportional to the inverse frequency. There have been no convincing VLBI observations to indicate a deviation from the scattering size at any frequency, however. One could also expect a change in in the centroid of emission that is comparable to the change in the source size. Astrometric experiments in the Galactic Center have achieved sub-mas accuracy (Reid et al. 1999).

The flux density of Sgr A* appears to decline on a timescale of 10 days. Synchrotron cooling is sufficient only for an ADAF model, where the cooling time at 15 GHz is 25 days. The low density model of Quataert & Gruzinov (2000a) and the jet model (Falcke & Markoff 2000) predict cooling times of ~ 200 days. Alfven velocities for the ADAF and Quataert & Gruzinov (2000a) model are on the order of $0.1cR^{-0.25}$, where R is the radius in units of the gravitational radius. The crossing time for a source 1 light-hour across would be about 1 day. For a jet model, the Alfven velocity is $\sim 0.5cR^{1/7}$. The crossing time would be about 1 hour, implying that continuous energization of the emitting region is necessary. This is not unreasonable given the substantial short-term variability seen at the peak of the flare.

We note also that the effects of scattering do not operate on a 10-d timescale. For a relative velocity $v = 100$ km s^{-1} between Earth and the scattering medium, we can calculate the diffractive and refractive timescales at 15 GHz. The diffractive timescale is ~ 3 s. The refractive timescale is ~ 2 y.

The similar LP and CP properties of M81* and Sgr A* suggest that there may be a class of low luminosity AGN with these polarization properties (Brunthaler et al. 2001). In addition to an absence of LP and the presence of CP (with a potentially inverted spectrum), the sources both show unusual inverted total intensity spectra. Such total intensity spectra are the result of inhomogeneous electron energy and magnetic field distributions.

10. Conclusions

We have presented here VLA and ATCA observations of CP and LP in Sgr A* that span timescales of 1 hour to 20 y at frequencies between 1.4 and 15 GHz. CP is clearly detected at all frequencies. In the short-term, it is variable with an increasing degree of variability with frequency. The average spectrum is inverted. In the long-term, the 4.8 GHz CP is

remarkably stable despite changes in total intensity. LP is not detected at any frequency.

We suggest that the CP has two separate components in frequency. A low frequency component peaks around 5 GHz and then decreases with $\alpha \sim -0.5$. A high frequency component is strongly variable. At maximum, the spectrum is inverted at 15 GHz with $\alpha \approx 1.5$ and $m_c \approx -1\%$. At minimum, the high frequency component disappears at the 0.1% level. The coincidence of the maximum in CP with a total intensity maximum suggests that these flaring events are related. The two component nature of the total intensity spectrum suggests that the higher frequency component may be $\sim 10\%$ circularly polarized at the flare peak.

Future millimeter wavelength observations of CP in Sgr A* can test this hypothesis. These observations should be timed to test the relationship between flaring in total intensity and in CP.

Finally, we note that these observations demonstrate the importance of CP for diagnosing the physics of compact radio sources. CP observations can constrain models for accretion, outflow and interstellar wave propagation.

The National Radio Astronomy Observatory is a facility of the National Science Foundation operated under cooperative agreement by Associated Universities, Inc. The Australia Telescope Compact Array is part of the Australia Telescope which is funded by the Commonwealth of Australia for operation as a National Facility managed by CSIRO.

REFERENCES

Agol, E. 2000, ApJ, 538, L121

Aitken, D. K., Greaves, J., Chrysostomou, A., Jenness, T., Holland, W., Hough, J. H., Pierce-Price, D., & Richer, J. 2000, ApJ, 534, L173

Backer, D. C. 1994, in NATO ASIC Proc. 445: The Nuclei of Normal Galaxies: Lessons from the Galactic Center, 403

Backer, D. C. & Sramek, R. A. 1999, ApJ, 524, 805

Baganoff, F. K., Bautz, M. W., Brandt, W. N., Chartas, G., Feigelson, E. D., Garmire, G. P., Maeda, Y., Morris, M., Ricker, G. R., Townsley, L. K., & Walter, F. 2001, Nature, 413, 45

Bower, G. C. & Backer, D. C. 1998, ApJ, 496, L97

Bower, G. C., Backer, D. C., Zhao, J. H., Goss, M., & Falcke, H. 1999a, ApJ, 521, 582

Bower, G. C., Falcke, H., & Backer, D. C. 1999b, ApJ, 523, L29

Bower, G. C., Wright, M. C. H., Backer, D. C., & Falcke, H. 1999c, ApJ, 527, 851

Bower, G. C., Wright, M. C. H., Falcke, H., & Backer, D. C. 2001, ApJ, 555, L103

Brunthaler, A., Bower, G. C., Falcke, H., & Mellon, R. R. 2001, ApJ, 560, L123

Coker, R., Melia, F., & Falcke, H. 1999, ApJ, 523, 642

Doeleman, S. S., Shen, Z.-Q., Rogers, A. E. E., Bower, G. C., Wright, M. C. H., Zhao, J. H., Backer, D. C., Crowley, J. W., Freund, R. W., Ho, P. T. P., Lo, K. Y., & Woody, D. P. 2001, AJ, 121, 2610

Duschl, W. J. & Lesch, H. 1994, A&A, 286, 431

Falcke, H. 1999, in ASP Conf. Ser. 186: The Central Parsecs of the Galaxy, 113

Falcke, H., Goss, W. M., Matsuo, H., Teuben, P., Zhao, J., & Zylka, R. 1998, ApJ, 499, 731

Falcke, H., Mannheim, K., & Biermann, P. L. 1993, A&A, 278, L1

Falcke, H. & Markoff, S. 2000, A&A, 362, 113

Fender, R., Rayner, D., Norris, R., Sault, R. J., & Pooley, G. 2000, ApJ, 530, L29

Fender, R. P., Rayner, D., McCormick, G., Muxlow, T. W. B., Pooley, G. G., Sault, R. J., & Spencer, R. E. 2001, MNRAS submitted

Frail, D. A., Diamond, P. J., Cordes, J. M., & van Langevelde, H. J. 1994, ApJ, 427, L43

Genzel, R., Pichon, C., Eckart, A., Gerhard, O. E., & Ott, T. 2000, MNRAS, 317, 348

Ghez, A. M., Morris, M., Becklin, E. E., Tanner, A., & Kremenek, T. 2000, Nature, 407, 349

Holdaway, M., Carilli, C., & Owen, F. 1992, VLA Sci., 163

Homan, D. C., Attridge, J. M., & Wardle, J. F. C. 2001, ApJ, 556, 113

Homan, D. C. & Wardle, J. F. C. 1999, AJ, 118, 1942

Hughes, P. A., Aller, H. D., & Aller, M. F. 1985, ApJ, 298, 301

—. 1992, ApJ, 396, 469

Jones, T. W. 1988, ApJ, 332, 678

Jones, T. W. & Odell, S. L. 1977, ApJ, 214, 522

Krichbaum, T. P., Graham, D. A., Witzel, A., Greve, A., Wink, J. E., Grewing, M., Colomer, F., de Vicente, P., Gomez-Gonzalez, J., Baudry, A., & Zensus, J. A. 1998, A&A, 335, L106

Lo, K. Y., Shen, Z. Q., Zhao, J. H., & Ho, P. T. P. 1998, ApJ, 508, L61

Macquart, J. . & Melrose, D. B. 2000, ApJ, 545, 798

Maoz, E. 1998, ApJ, 494, L181

Markoff, S., Falcke, H., Yuan, F., & Biermann, P. L. 2001, A&A, 379, L13

Marscher, A. P. & Gear, W. K. 1985, ApJ, 298, 114

Melia, F. 1994, ApJ, 426, 577

Melia, F. & Falcke, H. 2001, ARA&A, 39, 309

Melia, F., Liu, S., & Coker, R. 2000, ApJ, 545, L117

Özel, F., Psaltis, D., & Narayan, R. 2000, ApJ, 541, 234

Pacholczyk, A. G. 1977, Oxford Pergamon Press International Series on Natural Philosophy, 89

Quataert, E. & Gruzinov, A. 2000a, ApJ, 545, 842

—. 2000b, ApJ, 539, 809

Ramaty, R. 1969, ApJ, 158, 753

Rayner, D. P., Norris, R. P., & Sault, R. J. 2000, MNRAS, 319, 484

Reid, M. J., Readhead, A. C. S., Vermeulen, R. C., & Treuhaft, R. N. 1999, ApJ, 524, 816

Roberts, D. H., Wardle, J. F. C., & Brown, L. F. 1994, ApJ, 427, 718

Rogers, A. E. E., Doeleman, S., Wright, M. C. H., Bower, G. C., Backer, D. C., Padin, S., Philips, J. A., Emerson, D. T., Greenhill, L., Moran, J. M., & Kellermann, K. I. 1994, ApJ, 434, L59

Sault, R. J., Killeen, N. E. B., & Kesteven, M. J. 1991, AT Tech. Doc., 39.3/0.15

Sault, R. J. & Macquart, J.-P. 1999, ApJ, 526, L85

Sault, R. J., Teuben, P. J., & Wright, M. C. H. 1995, in ASP Conf. Ser. 77: Astronomical Data Analysis Software and Systems IV, Vol. 4, 433

Serabyn, E., Carlstrom, J., Lay, O., Lis, D. C., Hunter, T. R., & Lacy, J. H. 1997, ApJ, 490, L77

Wardle, J. F. C., Homan, D. C., Ojha, R., & Roberts, D. H. 1998, Nature, 395, 457

Weiler, K. W. & de Pater, I. 1983, ApJS, 52, 293

Zhao, J., Bower, G. C., & Goss, W. M. 2001, ApJ, 547, L29

Zhao, J., Goss, W. M., Lo, K.-Y., & Ekers, R. D. 1992, in ASP Conf. Ser. 31: Relationships Between Active Galactic Nuclei and Starburst Galaxies, 295

AAS LaTeX macros v5.0.

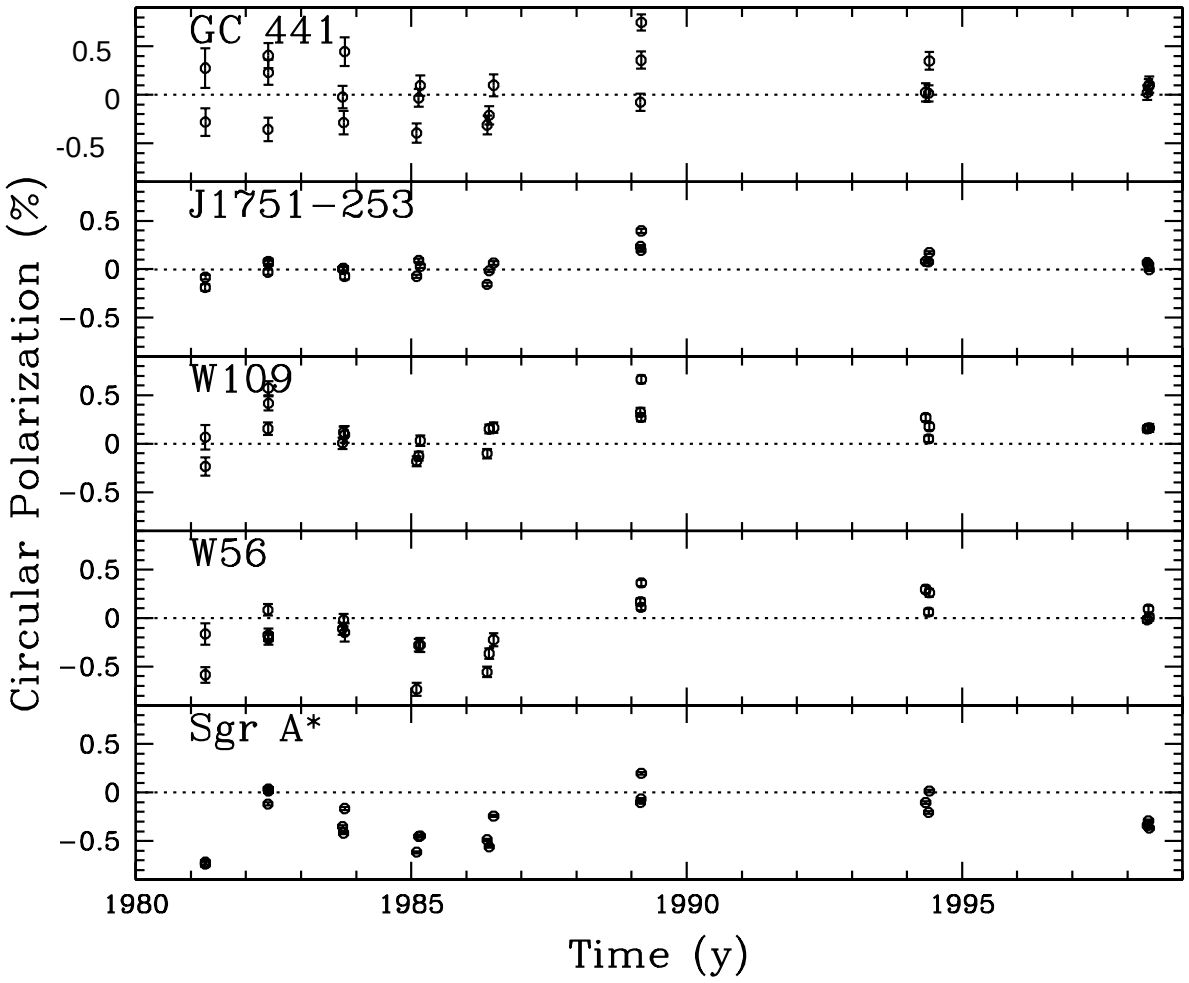

Fig. 1.— Raw fractional CP for five sources with 4.8 GHz data taken from the VLA archives. Error bars represent thermal noise.

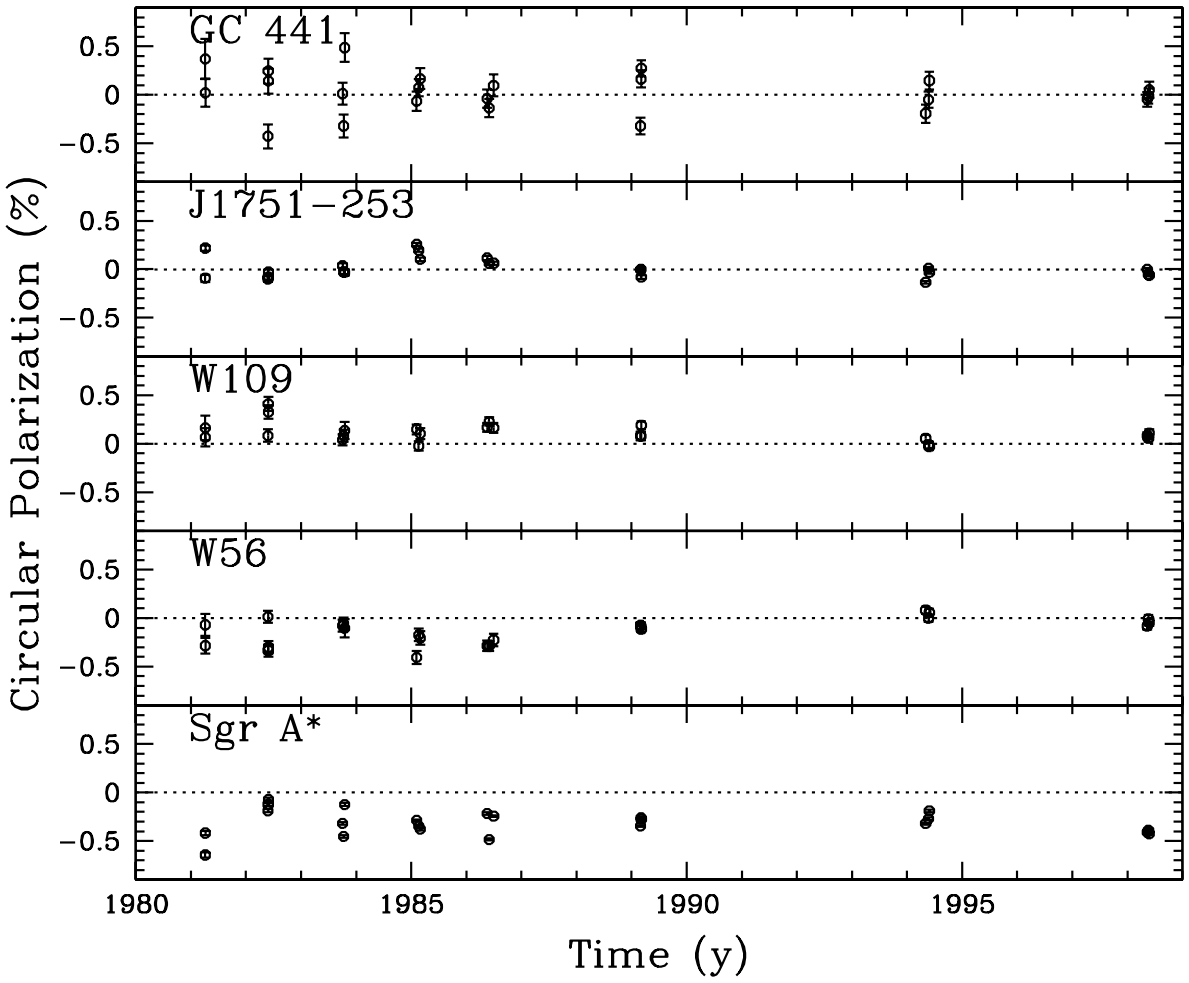

Fig. 2.— Corrected fractional CP for five sources with 4.8 GHz data taken from the VLA archives

.

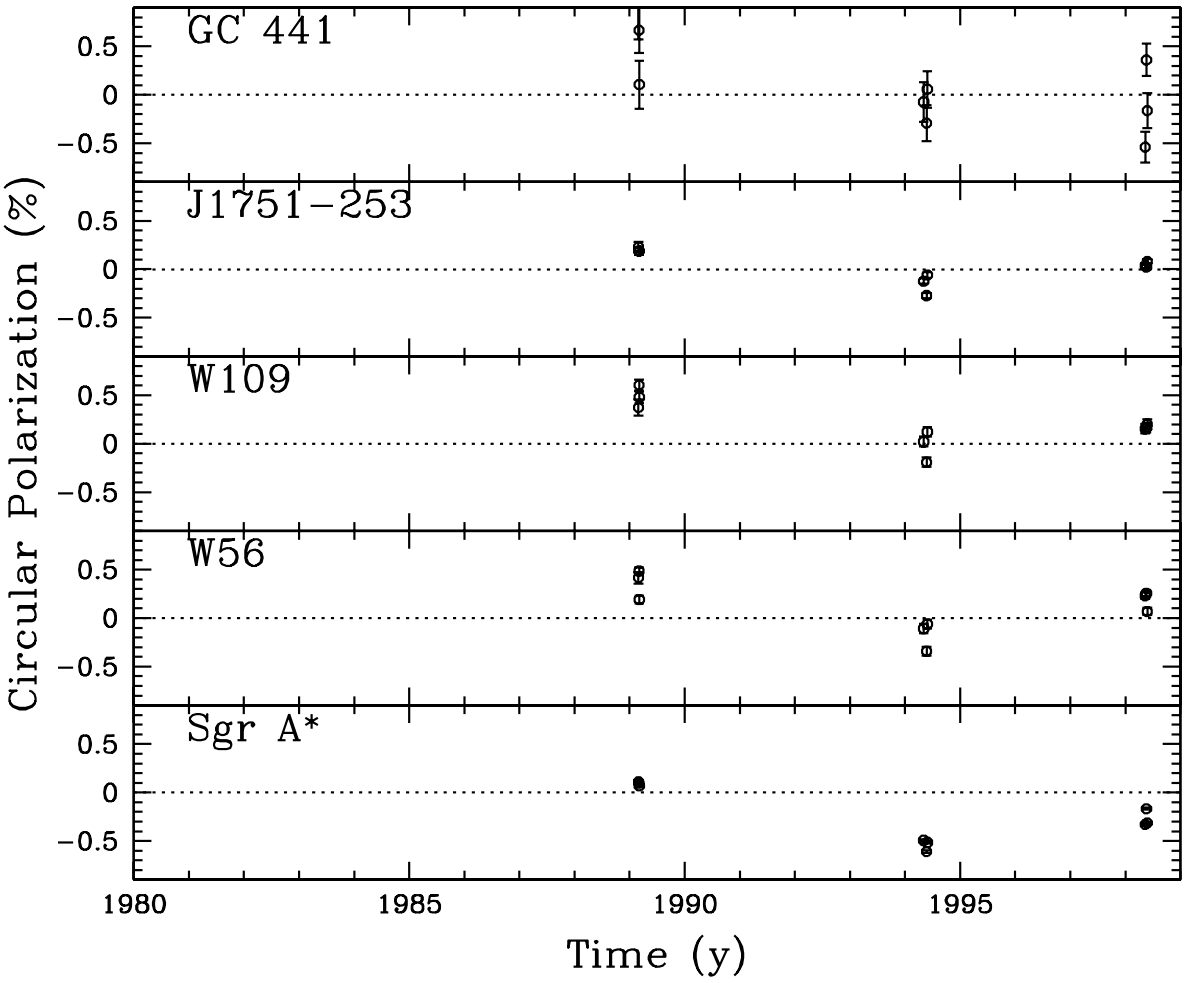

Fig. 3.— Raw fractional CP for five sources with 8.4 GHz data taken from the VLA archives. Error bars represent thermal noise.

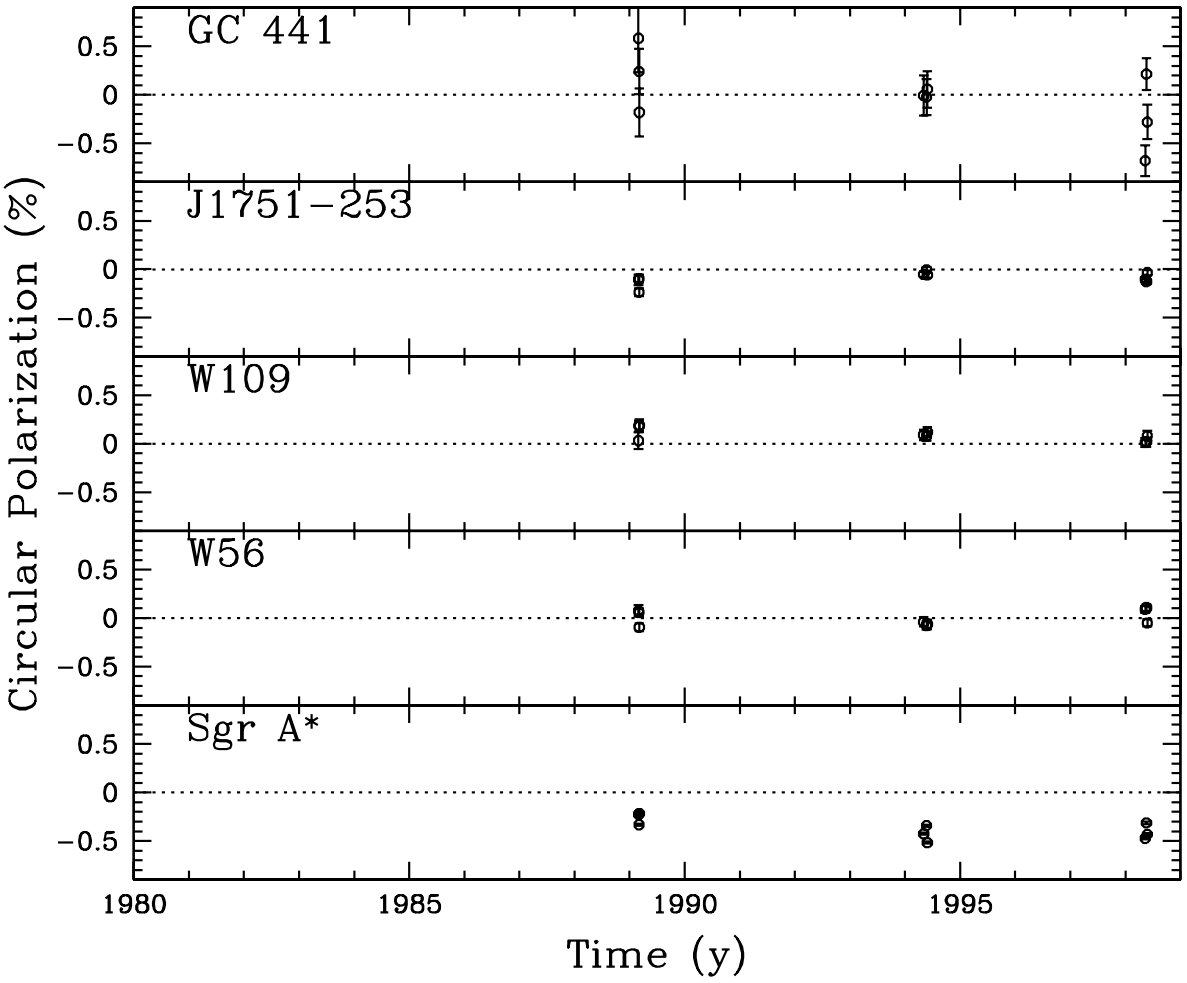

Fig. 4.— Corrected fractional CP for five sources with 8.4 GHz data taken from the VLA archives

.

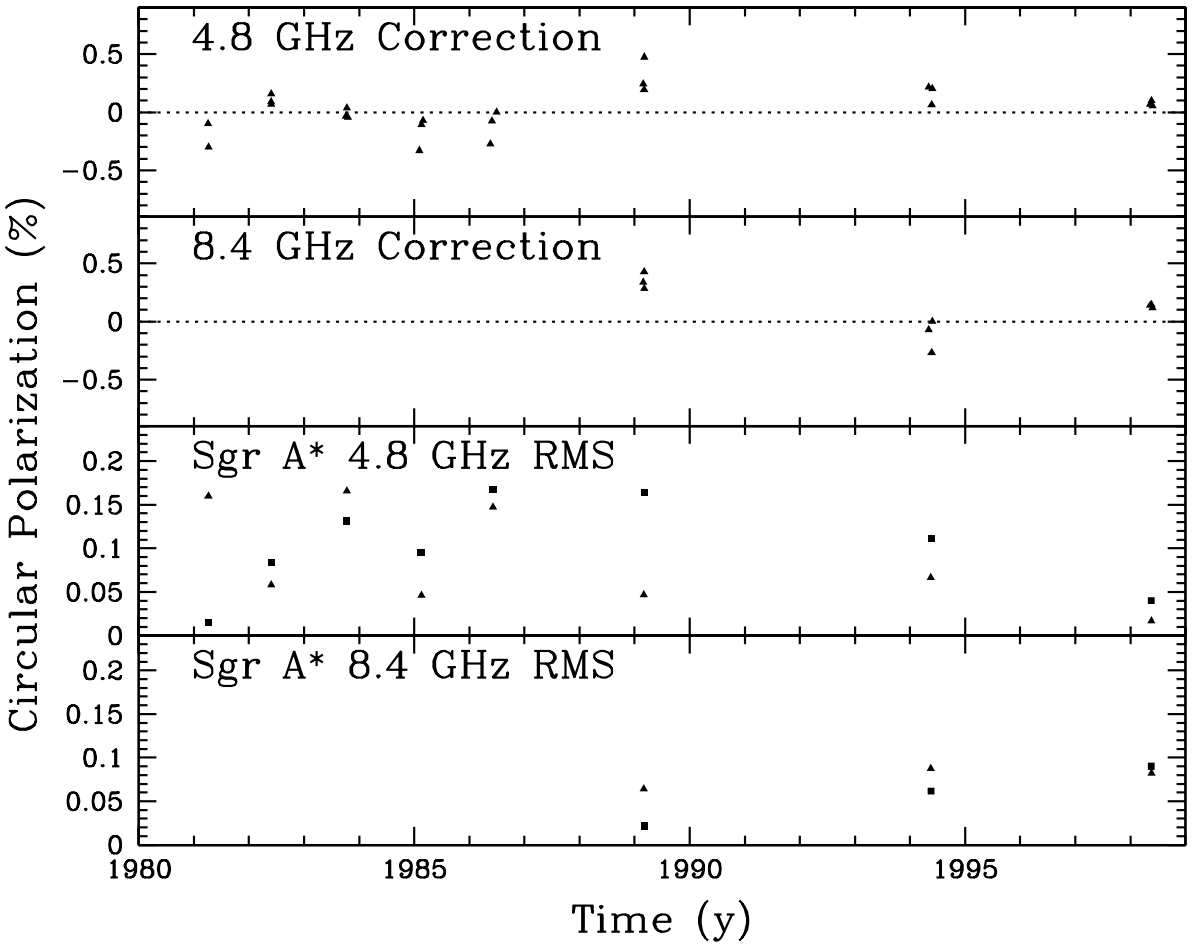

Fig. 5.— Correction terms for the raw fractional CP at 4.8 GHz (top panel) and at 8.4 GHz (second from top panel) and their effect on the rms scatter for Sgr A* within epochs at 4.8 GHz (second from bottom panel) and at 8.4 GHz (bottom panel). Triangles in the bottom panels represent corrected data. Squares represent uncorrected data.

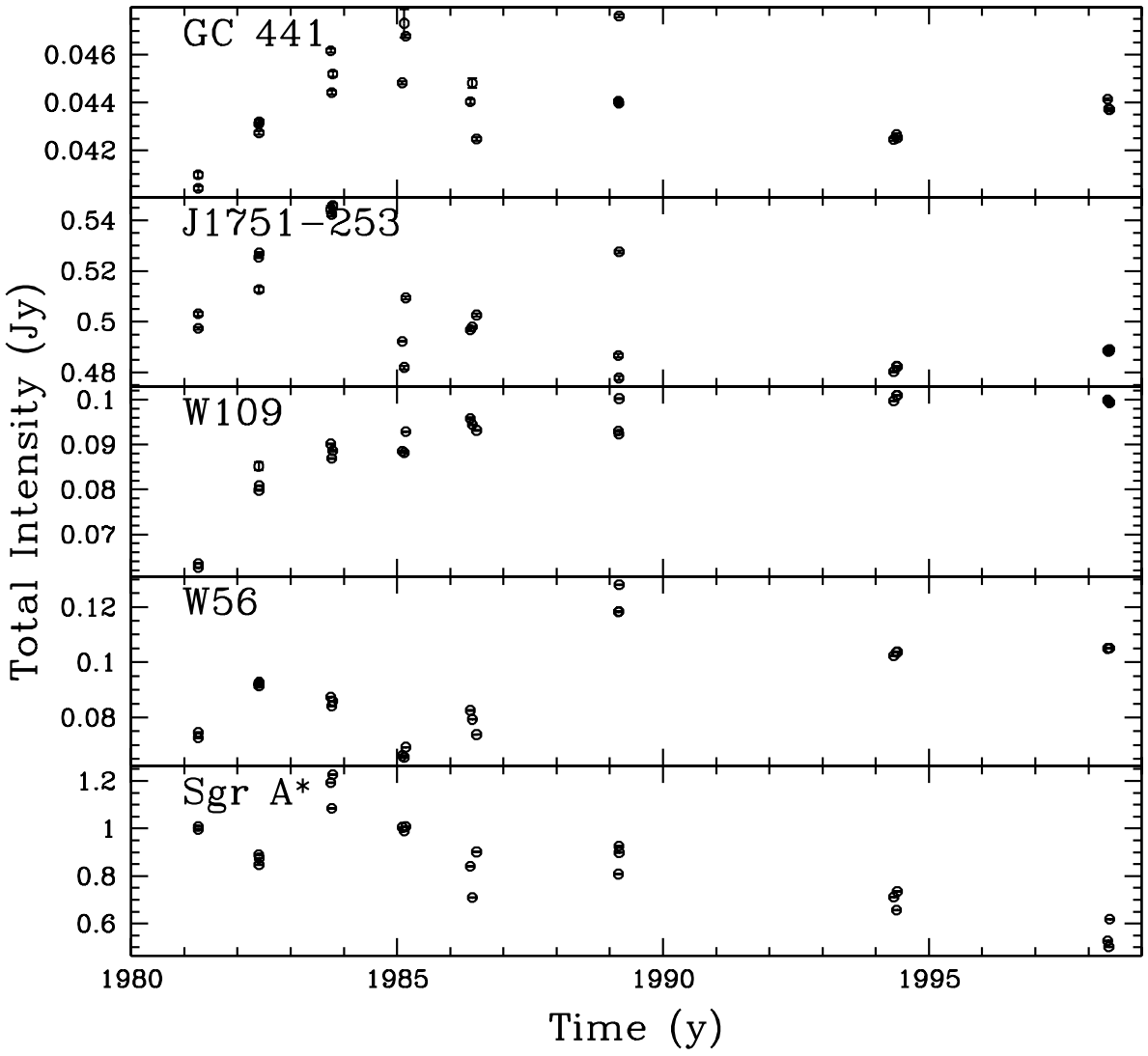

Fig. 6.— Total intensity for five sources with 4.8 GHz data taken from the VLA archives.

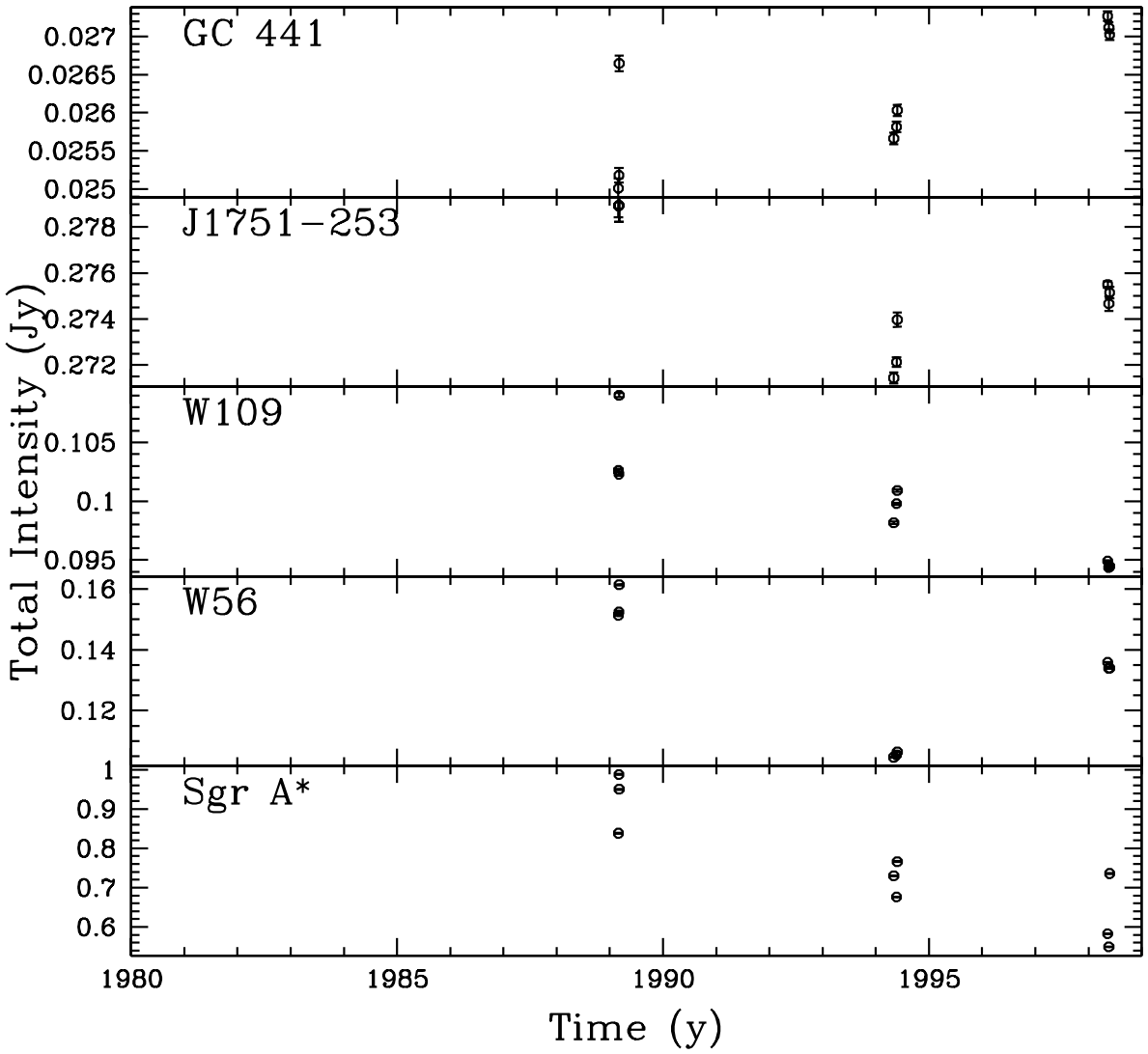

Fig. 7.— Total intensity for five sources with 8.4 GHz data taken from the VLA archives.

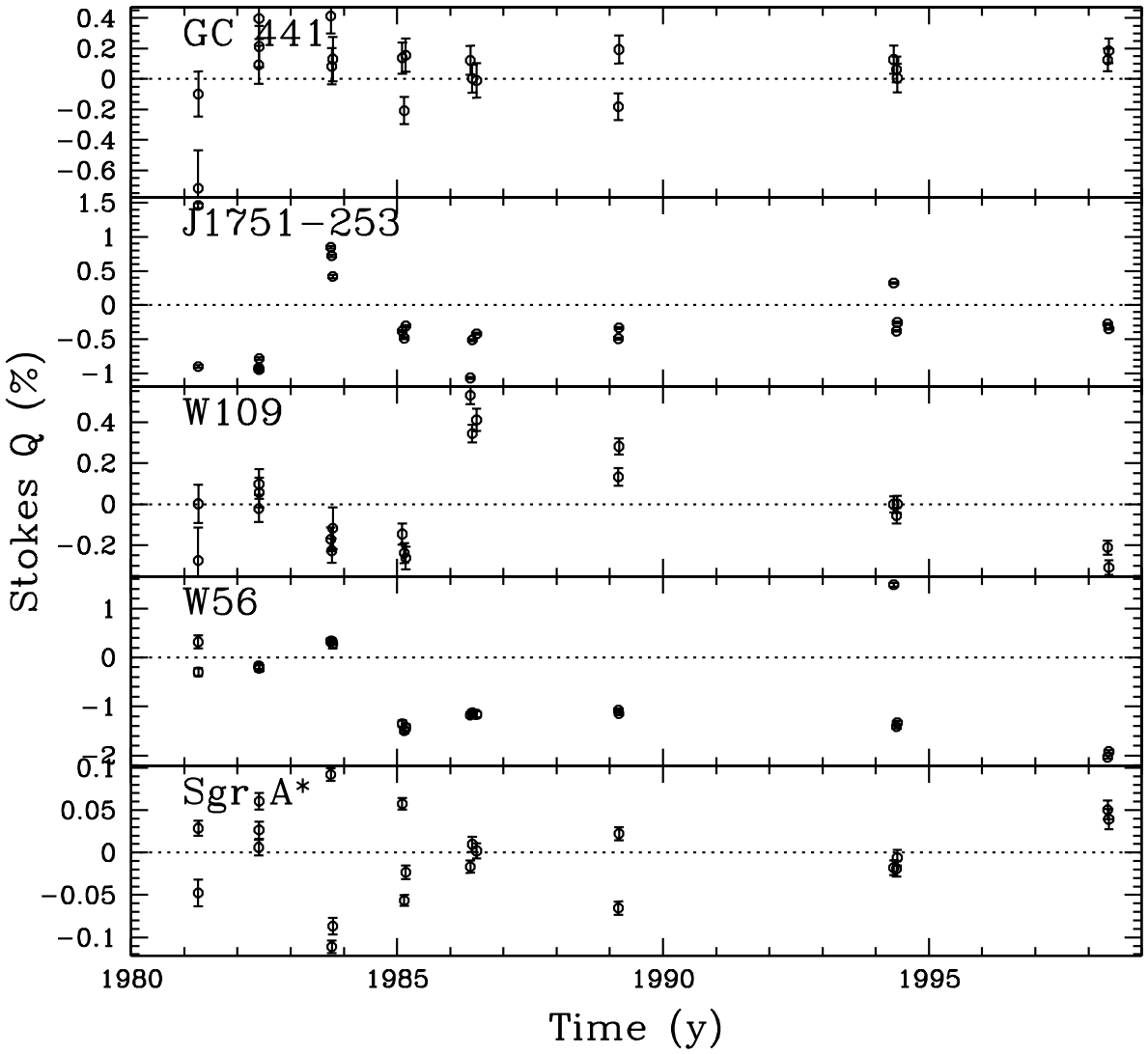

Fig. 8.— Fractional Stokes Q for five sources with 4.8 GHz data taken from the VLA archives.

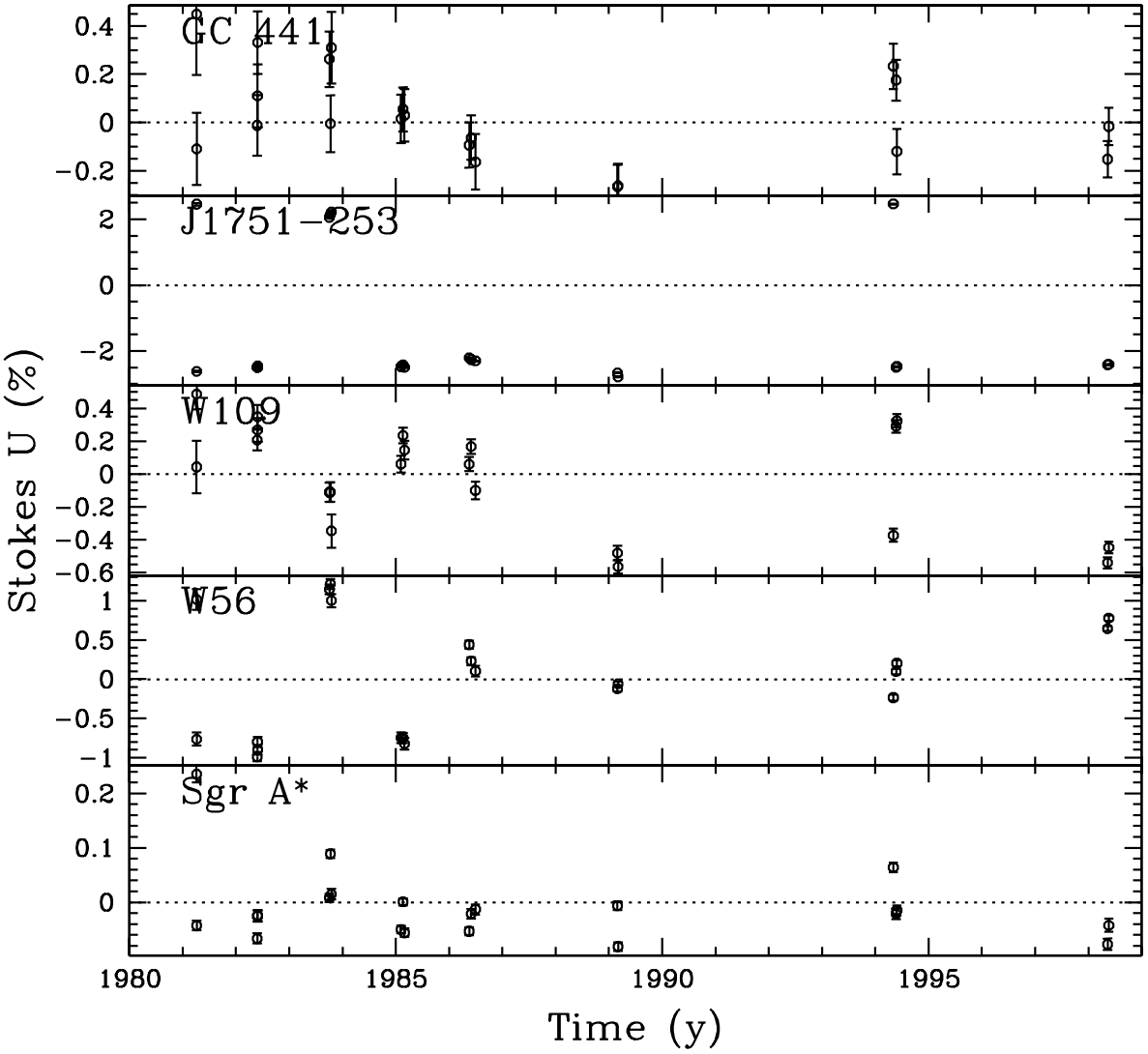

Fig. 9.— Fractional Stokes U for five sources with 4.8 GHz data taken from the VLA archives.

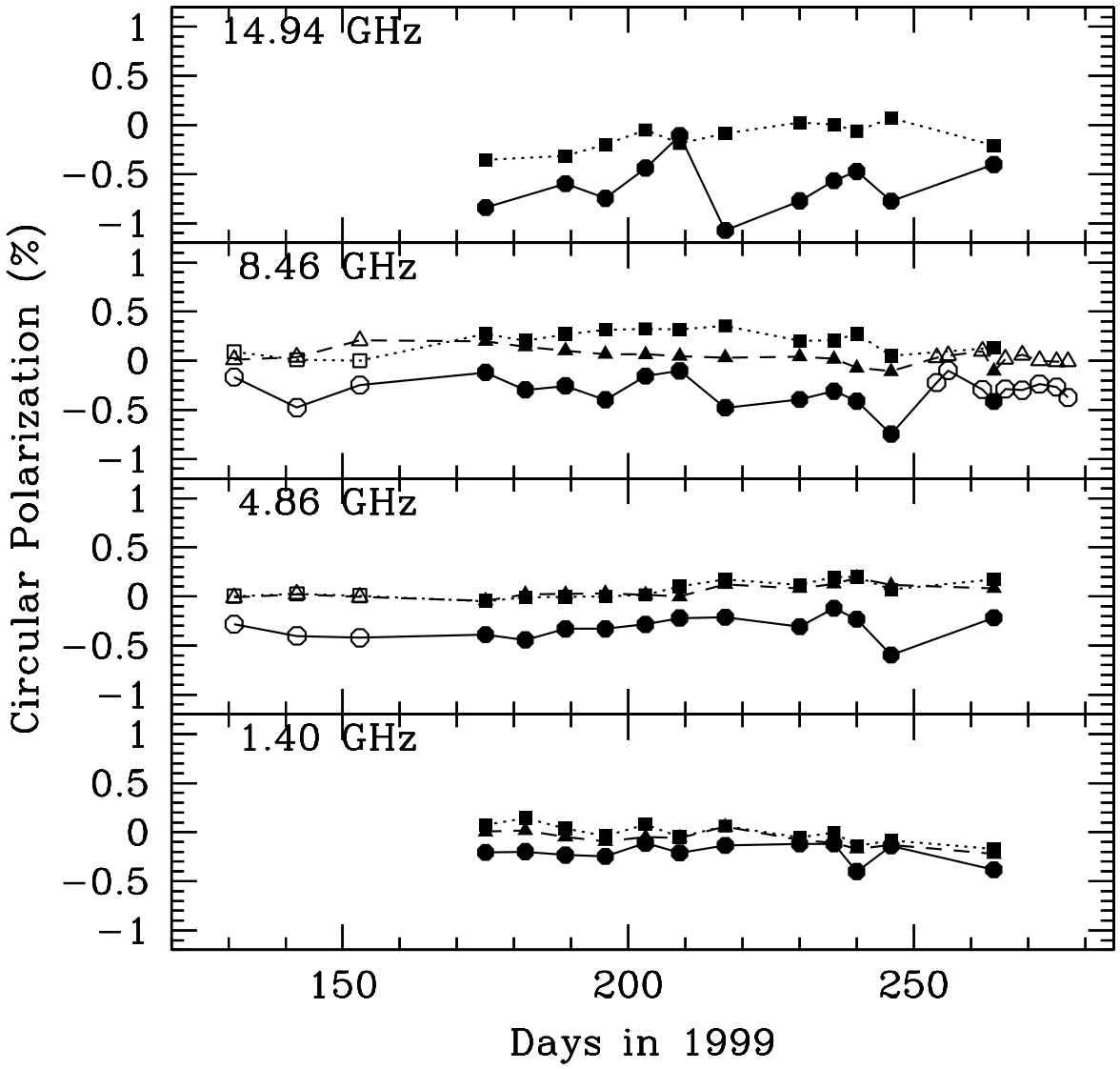

Fig. 10.— Fractional CP for three sources at 1.4, 4.8, 8.4 and 14.9 GHz from the 1999 VLA and ATCA monitoring campaigns. Octagons and solid lines are for Sgr A*, squares and short-dashed lines are for J1744-3116, and triangles and long-dashed lines are for J1751-2523. Solid symbols are for the VLA and open symbols are for ATCA.

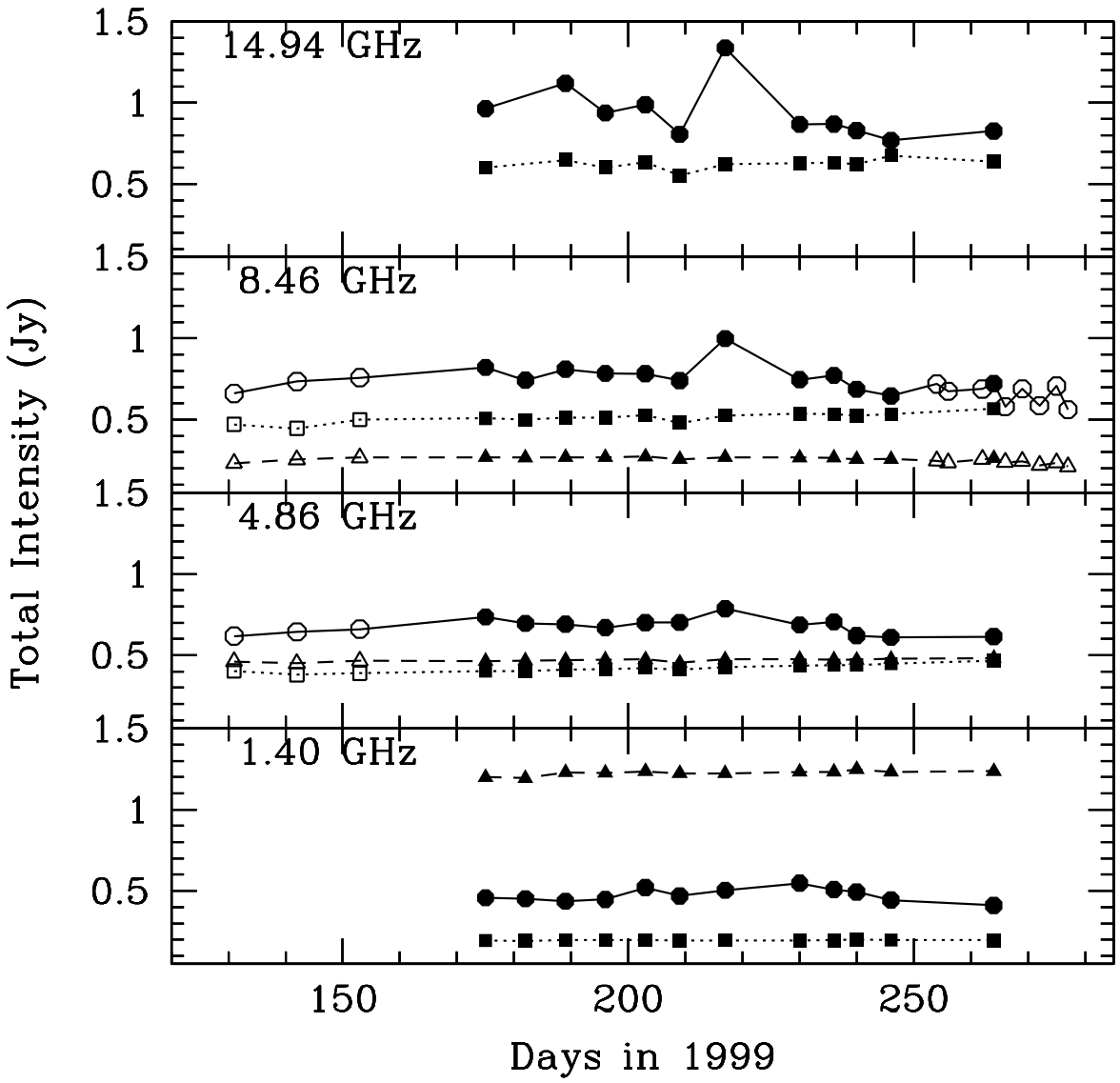

Fig. 11.— Total intensity for three sources at 1.4, 4.8, 8.4 and 14.9 GHz from the 1999 VLA and ATCA monitoring campaigns. Symbols are the same as in Figure 10.

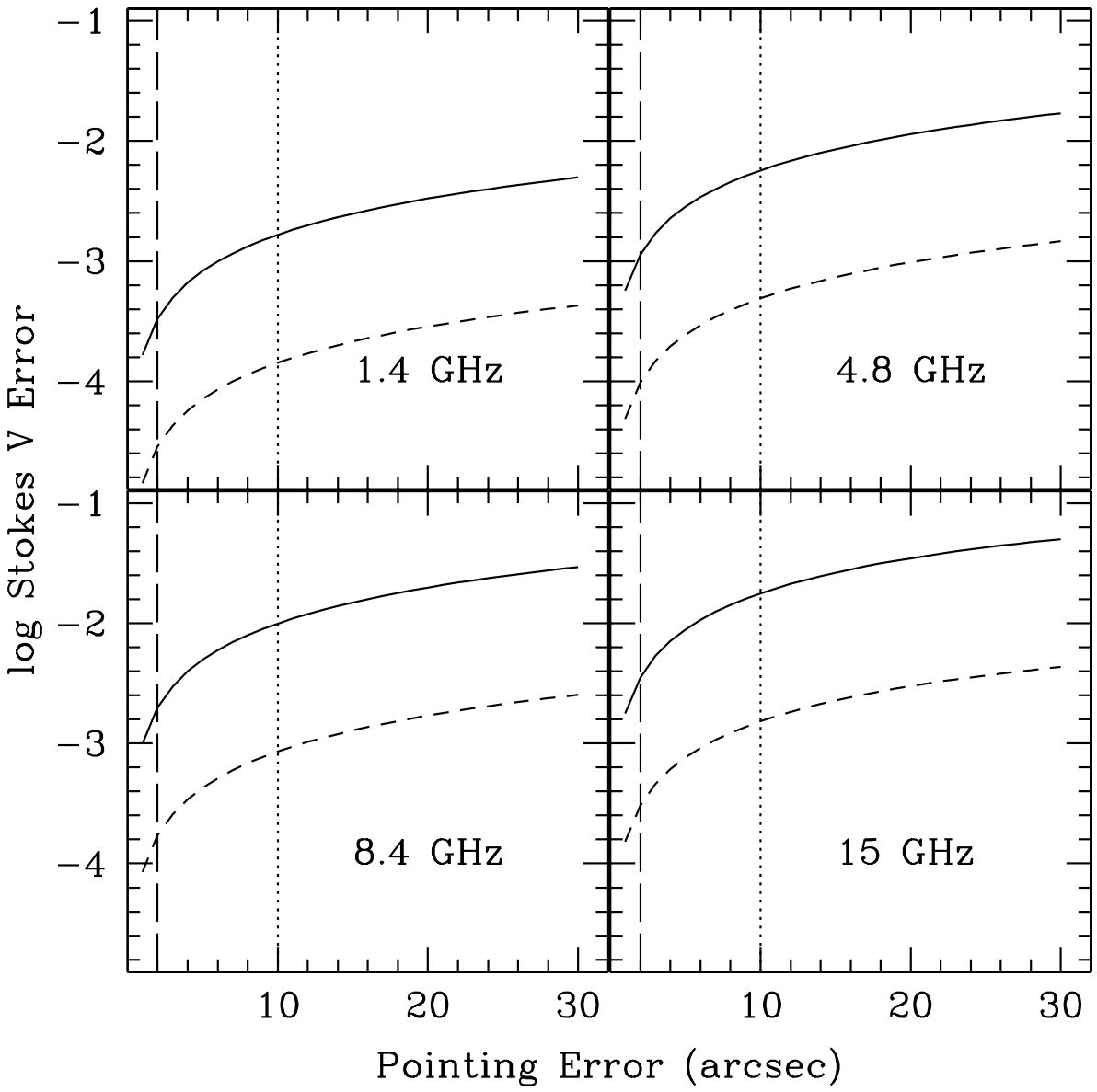

Fig. 12.— The fractional error due to beam squint at four frequencies. The solid curve is the error from a single antenna and the short-dashed curve is the error from 27 antennas with 5 observations. The dotted vertical line is the expected rms pointing error without pointing observations. The long-dashed vertical line is the best-case rms pointing error with pointing observations.

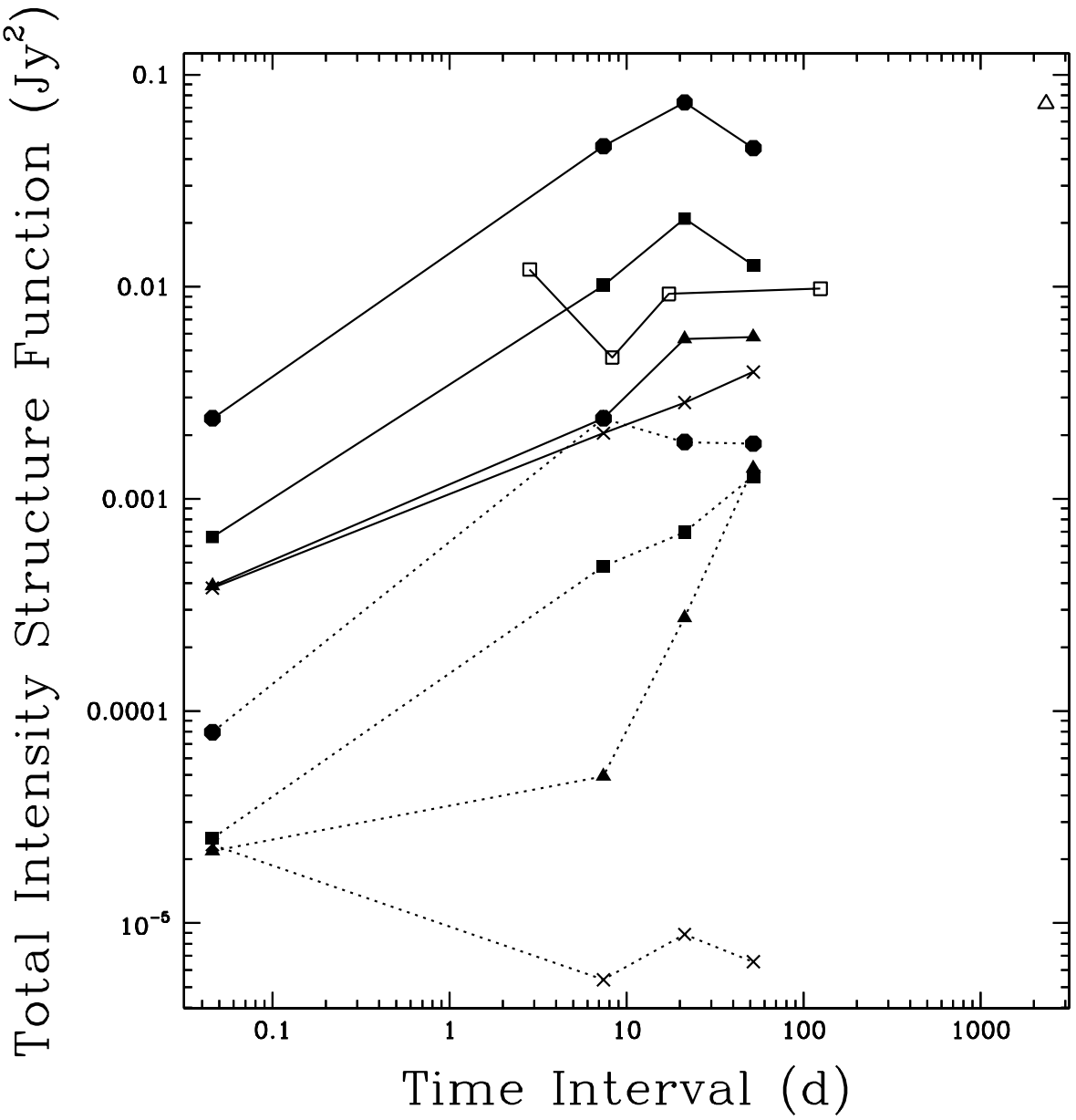

Fig. 13.— The structure function of the total intensity for Sgr A* (connected by solid lines) and J1744-3116 (connected by dotted lines) from VLA and ATCA measurements. The structure function derived solely from VLA measurements in 1999 is indicated with crosses (1.4 GHz), filled triangles (4.8 GHz), filled squares (8.4 GHz) and filled octagons (15 GHz). The structure function derived from VLA archive data at 4.8 GHz is indicated with an open triangle. The structure function derived from ATCA measurements at 8.4 GHz is indicated with open squares. Errors for individual structure function measurements are on the order

of a factor of two.

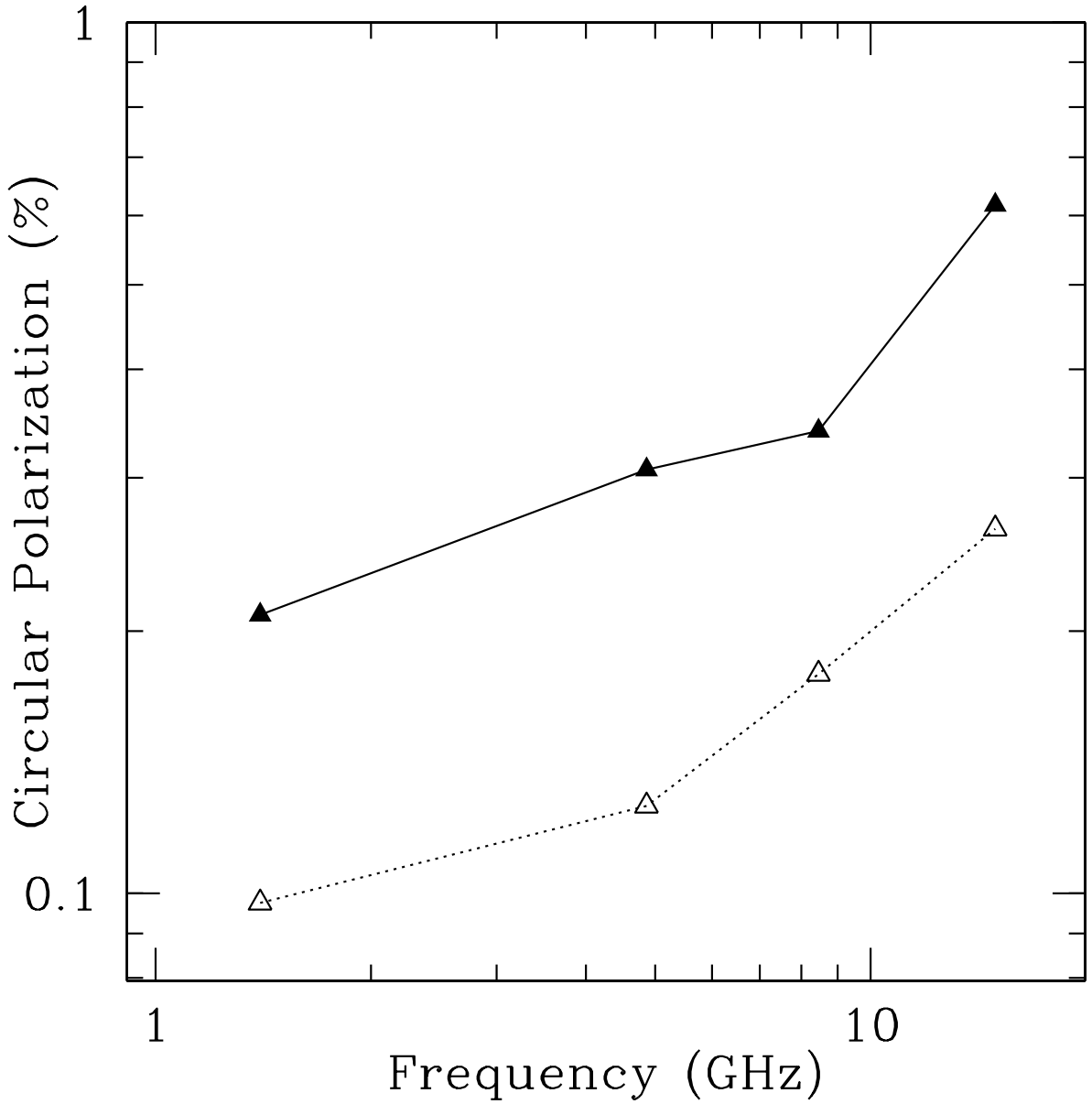

Fig. 14.— The mean spectrum (solid triangles) and degree of variability (open triangles) of fractional CP in Sgr A* as a function of frequency.

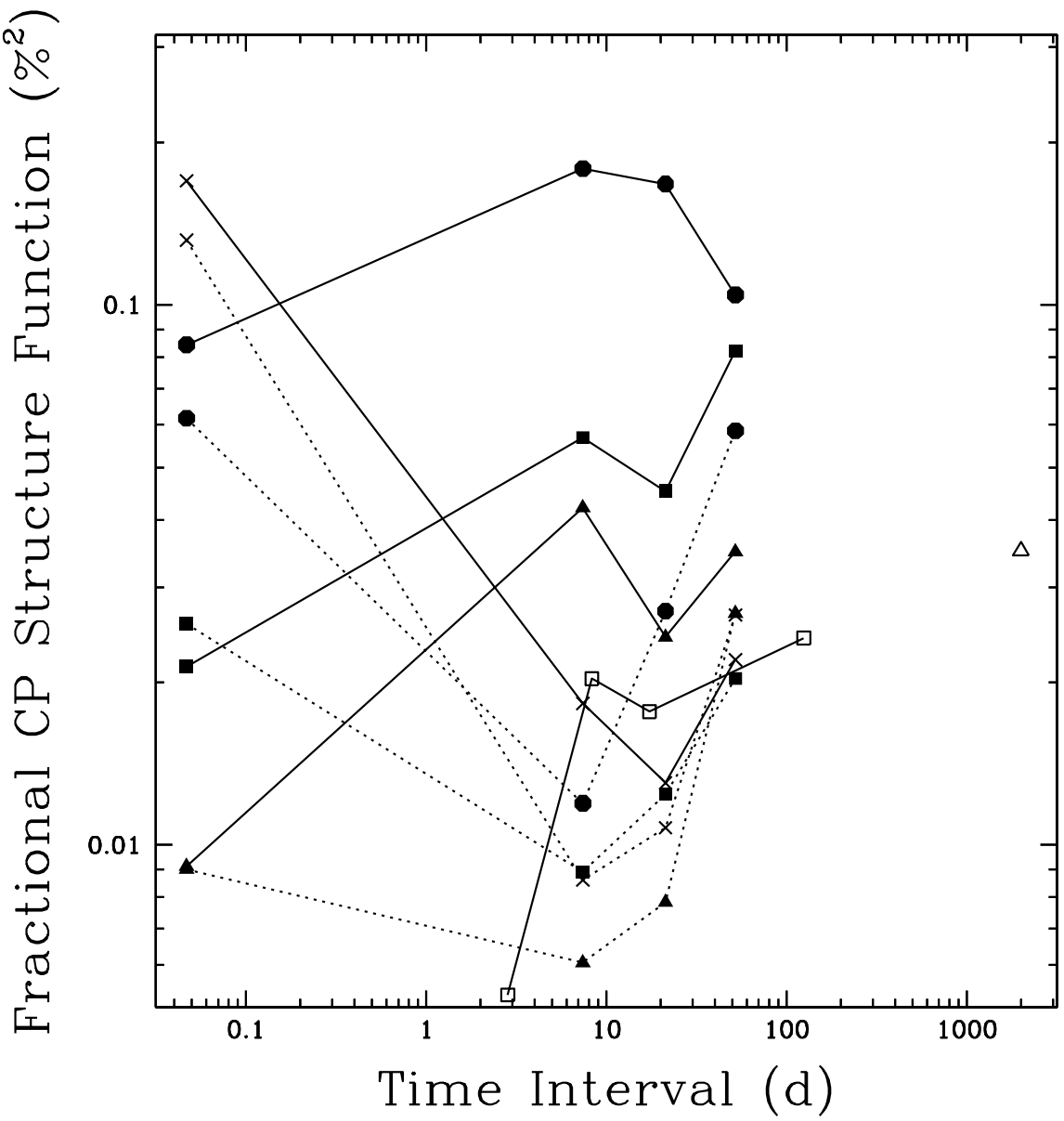

Fig. 15.— The structure function of fractional CP for Sgr A* and J1744-3116 from VLA and ATCA measurements. The units of fractional CP are in percent. Thus, a difference of 0.1% corresponds to a structure function value of 0.01. Symbols are the same as in Figure 13. Errors for individual structure function measurements are on the order of a factor of two.

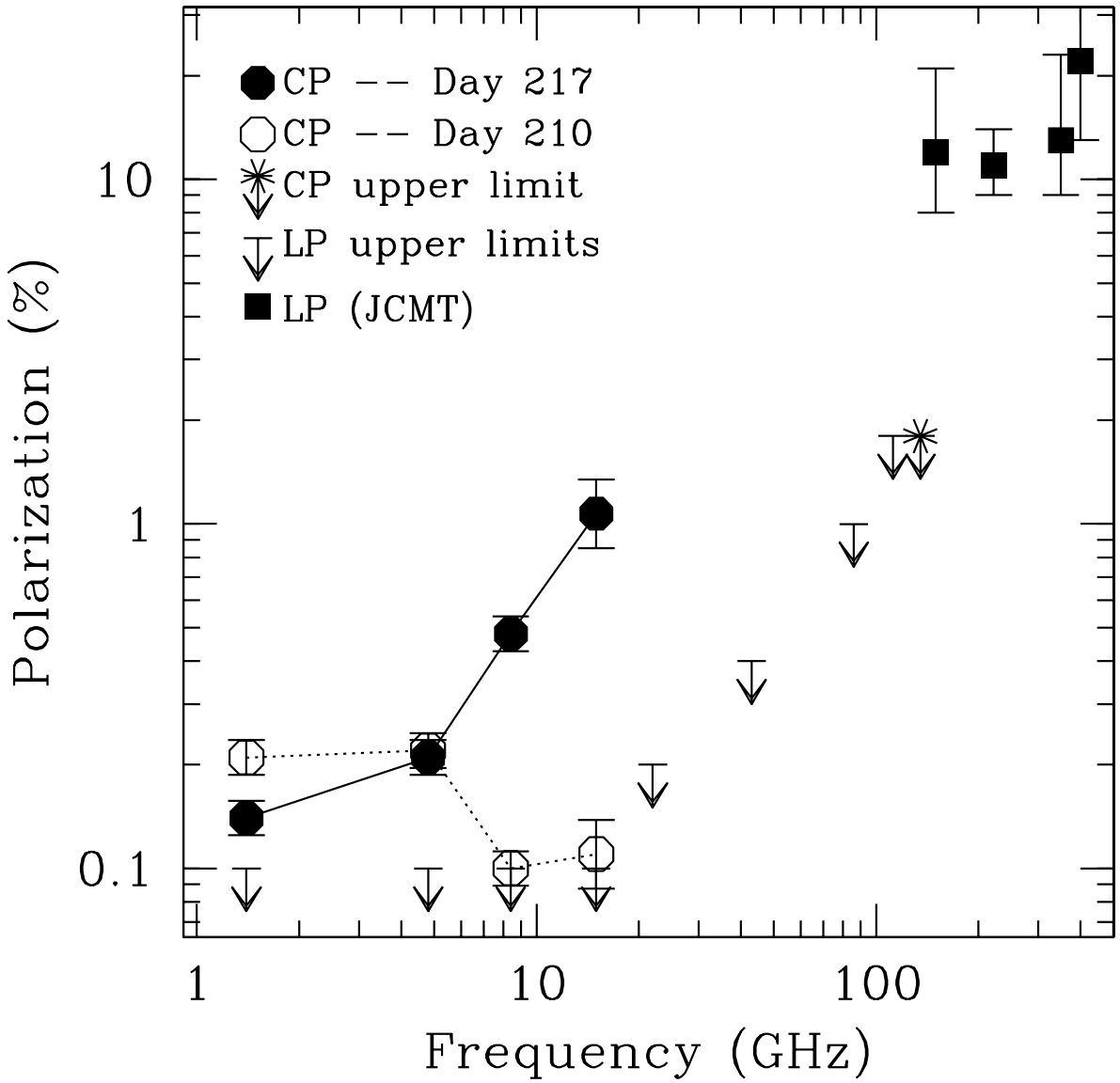

Fig. 16.— The spectrum of CP in Sgr A* from VLA measurements on day 210 (open octagons) and day 217 (filled octagons). We also include an upper limit for CP from BIMA at 112 GHz (Bower et al. 2001). LP upper limits and reported JCMT detections (squares) are also plotted. The sign of the CP has been reversed for clarity.

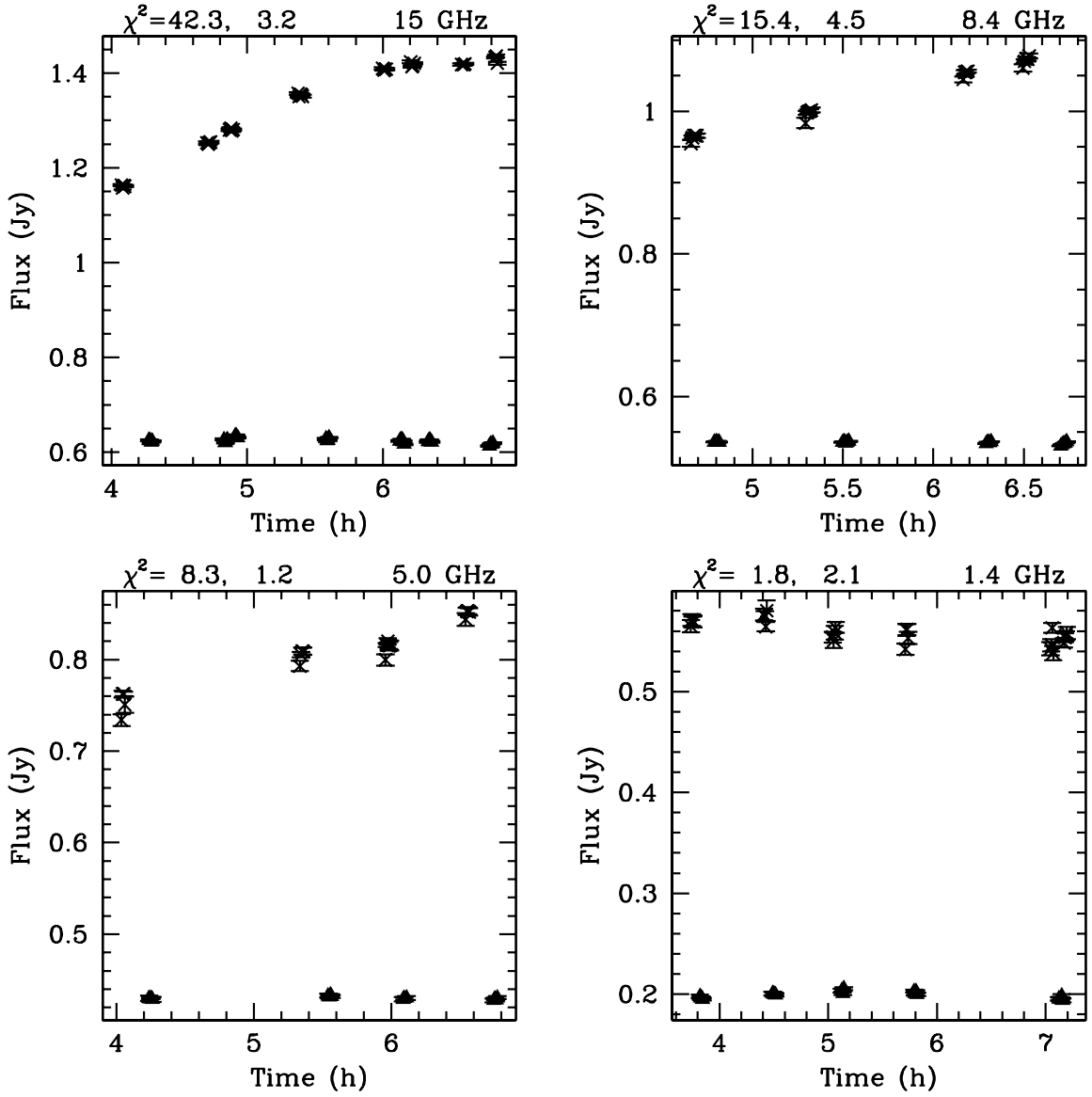

Fig. 17.— Short time scale variations in total intensity for Sgr A* (crosses) and J1744-3116 (triangles) at 1.4, 4.8, 8.4 and 15 GHz from VLA observations on day 217. The reduced χ^2 for the hypothesis of constant flux density is listed in each box for Sgr A* and J1744-3116, respectively.

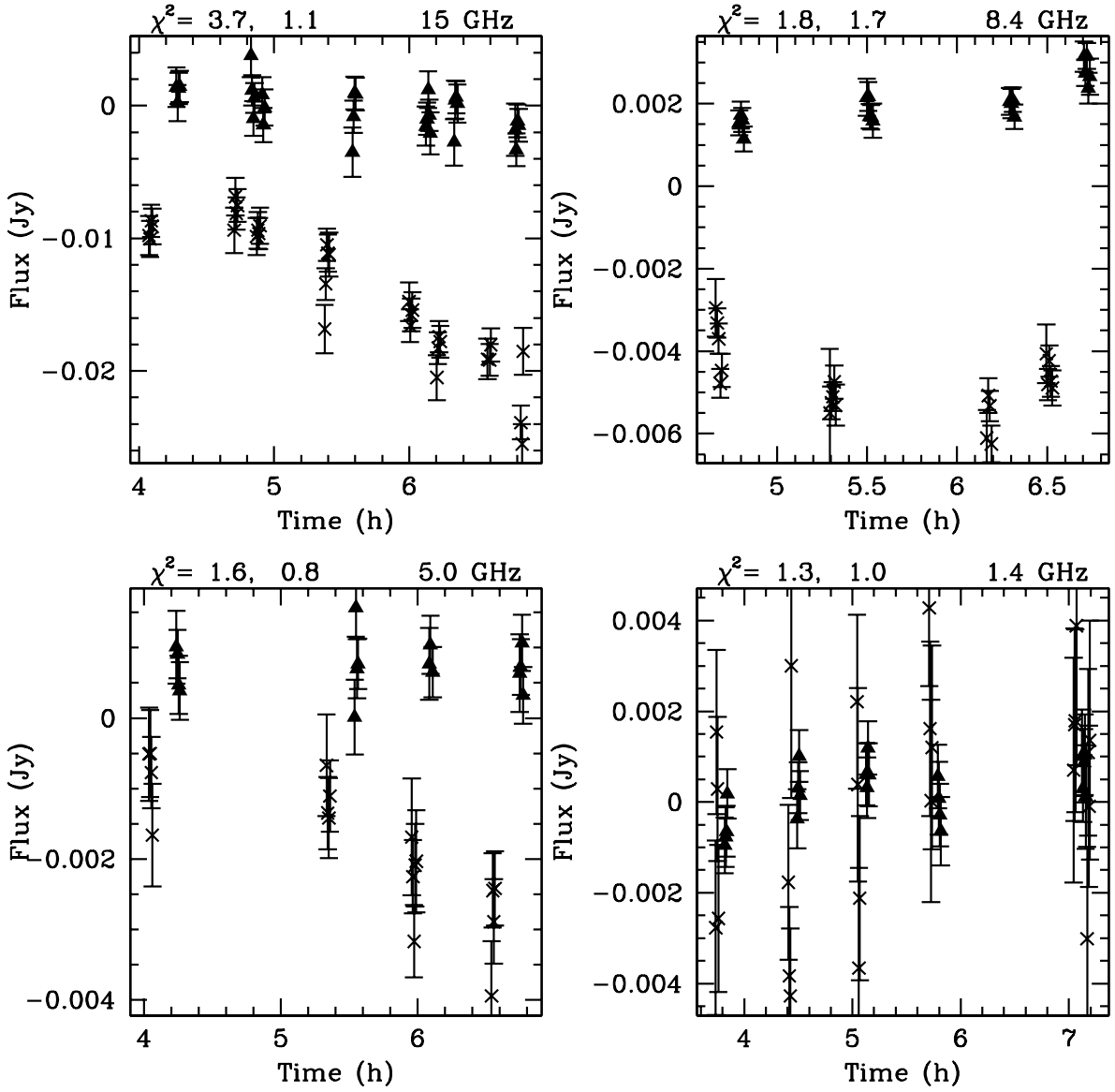

Fig. 18.— Short time scale variations in circular polarization for Sgr A* (crosses) and J1744-3116 (triangles) at 1.4, 4.8, 8.4 and 15 GHz from VLA observations on day 217. The reduced χ^2 for the hypothesis of constant flux density is listed in each box for Sgr A* and J1744-3116, respectively.

Table 1. Mean Total Intensity (Jy)

Source	Obs.	1.4 GHz	4.8 GHz	8.4 GHz	15 GHz
Sgr A*	VLA 1999	0.474 ± 0.040	0.685 ± 0.051	0.773 ± 0.091	0.937 ± 0.166
	ATCA 1999	...	0.641 ± 0.022	0.669 ± 0.065	...
	VLA Arch	...	0.868 ± 0.191	0.757 ± 0.149	...
J1744-3116	VLA 1999	0.196 ± 0.002	0.427 ± 0.023	0.520 ± 0.030	0.623 ± 0.031
	ATCA 1999	...	0.391 ± 0.012	0.473 ± 0.028	...
J1751-2523	VLA 1999	1.226 ± 0.015	0.472 ± 0.007	0.264 ± 0.006	...
	ATCA 1999	...	0.459 ± 0.008	0.240 ± 0.016	...
	VLA Arch	...	0.504 ± 0.022	0.276 ± 0.003	...
J1820-2528	ATCA 1999	...	1.033 ± 0.007	1.025 ± 0.062	...
J1733-1304	ATCA 1999	...	4.346 ± 0.552	3.798 ± 0.257	...
J1743-038	ATCA 1999	...	4.842 ± 0.528	4.110 ± 0.104	...
W56	ATCA 1999	...	0.092 ± 0.004	0.111 ± 0.006	...
	VLA Arch	...	0.092 ± 0.018	0.132 ± 0.022	...
W109	ATCA 1999	...	0.085 ± 0.002	0.070 ± 0.003	...
	VLA Arch	...	0.090 ± 0.011	0.100 ± 0.005	...
GC 441	ATCA 1999	...	0.042 ± 0.002	0.023 ± 0.002	...
	VLA Arch	...	0.044 ± 0.002	0.026 ± 0.001	...

Table 2. Mean Fractional CP (%)

Source	Obs.	1.4 GHz	4.8 GHz	8.4 GHz	15 GHz
Sgr A*	VLA 1999	-0.21 ± 0.10	-0.31 ± 0.13	-0.34 ± 0.18	-0.62 ± 0.26
	ATCA 1999	...	-0.37 ± 0.08	-0.27 ± 0.10	...
	VLA Arch	...	-0.31 ± 0.13	-0.36 ± 0.10	...
J1744-3116	VLA 1999	-0.01 ± 0.09	-0.08 ± 0.09	0.24 ± 0.09	-0.12 ± 0.14
	ATCA 1999	...	0.01 ± 0.01	0.04 ± 0.05	...
J1751-2523	VLA 1999	-0.08 ± 0.08	0.06 ± 0.07	0.04 ± 0.09	...
	ATCA 1999	...	0.00 ± 0.02	0.05 ± 0.06	...
J1820-2528	ATCA 1999	...	-0.08 ± 0.01	0.08 ± 0.04	...
J1733-1304	ATCA 1999	...	-0.14 ± 0.09	-0.10 ± 0.06	...
J1743-0350	ATCA 1999	...	-0.10 ± 0.02	-0.01 ± 0.05	...
W56	ATCA 1999	...	0.13 ± 0.05	0.22 ± 0.11	...
W109	ATCA 1999	...	0.00 ± 0.06	-0.07 ± 0.08	...
GC 441	ATCA 1999	...	0.01 ± 0.08	0.13 ± 0.41	...

Table 3. Estimated Errors in Fractional CP (%)

ν (GHz)	Thermal	Beam Sq.	Gain	D-terms	Total ($N = 5$)
1.4	$0.02/\sqrt{N}$	$0.04/\sqrt{N}$	$0.06/\sqrt{N}$	0.03	0.05
4.8	$0.02/\sqrt{N}$	$0.04/\sqrt{N}$	$0.06/\sqrt{N}$	0.03	0.05
8.4	$0.02/\sqrt{N}$	$0.04/\sqrt{N}$	$0.06/\sqrt{N}$	0.03	0.05
15	$0.05/\sqrt{N}$	$0.07/\sqrt{N}$	$0.06/\sqrt{N}$	0.03	0.06

Table 4. Point-by-Point Variations in Measured VLA Fractional CP(%)

ν (GHz)	Sgr A*	J1751-2523	J1744-3116
1.4	0.15	0.07	0.10
4.8	0.19	0.06	0.07
8.4	0.22	0.03	0.10
15	0.42	...	0.14